TIME-DEPENDENT SEISMIC PERFORMANCE ASSESSMENT OF RC BUILDINGS EXPOSED TO CORROSION

by

Hüseyin Çolak

B.S., Civil Engineering, Bogazici University, 2013

M.S., Civil Engineering, Bogazici University, 2016

Submitted to the Institute for Graduate Studies in
Science and Engineering in partial fulfillment of
the requirements for the degree of
Doctor of Philosophy

Graduate Program in Civil Engineering

Boğaziçi University

2023

to my parents &

to my beloved wife

ACKNOWLEDGEMENTS

I would like to express my heartfelt gratitude and reverence to my thesis supervisor, Prof. Serdar Soyöz, for his leading me into this research area almost ten years ago, and offering me this precious opportunity. I would like to thank him for his continuous guidance and advice throughout my graduate studies. I could not have asked for better inspiration, support, and patient.

I would like to thank to my thesis monitoring committee members, Prof. Kutay Orakçal and Assoc. Prof. Ufuk Yazgaz. Their suggestions and our discussions during the thesis progress meetings have improved the quality of this study significantly.

I am also thankful to my committee members, Prof. Hilmi Luş and Assoc. Prof. Barlas Özden Çağlayan for their attention, time, and valuable suggestions.

I would like to express my gratitude to Dr. Sunil Nataraj, Dr. Lucas Hogan, Assoc. Prof. Allan Scott and Prof. Jason Ingham for their permission and providing information about the case study building.

I should also thank to my talented friends, Emre Aytulun and Oğuz Şenkardeşler, who have kindly supported me in this journey. It was always delicious to discuss different aspects of this study with them.

I would like to show my deepest appreciation to my parents for their unconditional love and emotional encouragement throughout my life.

Last but not least, I would like to thank to my beloved wife, Merve. It was the toughest few years of my life and her support, patience and love helped me more than she knows. It was wonderful to walk together on our PhD journeys.

ABSTRACT

TIME-DEPENDENT SEISMIC PERFORMANCE ASSESSMENT OF RC BUILDINGS EXPOSED TO CORROSION

Corrosion of reinforcing bars is one of the most notable reasons of the deterioration of reinforced concrete structures. The safety problems related to corrosion and the differences between the required and available budgets that will be used to repair the existing structures make the reliable prediction of the service-life of structures quite critical to optimize the costs by accurately prioritizing the rehabilitation projects and to overcome the structural safety problems. In this study, Reverse Monte Carlo method is used to predict the future corrosion propagation of existing structures in accordance with the existing corrosion levels identified by site inspections. The novelty of the proposed method is to use existing corrosion levels of the reinforcements to increase the reliability of the expectations related to corrosion propagation in the future. In other words, site measurements are used as reference points according to which mathematical models used to predict corrosion levels can be validated. A case study was performed using the proposed method for a corroded reinforced concrete building located in New Zealand and constructed in 1928. As the first step, the existing corrosion level of the building was used to predict how corrosion can propagate in the future. Afterwards, the finite element model of the building was developed using the OpenSees platform, and nonlinear static analyses were performed to assess the future seismic performance of the building. Results shows that the data of the existing corrosion levels of a building can be a valuable input to make reliable estimations for the future seismic performances of the existing buildings.

ÖZET

KOROZYONA MARUZ KALAN BETONARME BİNALARIN ZAMANA BAĞLI SİSMİK PERFORMANS DEĞERLENDİRMESİ

Donatı çubuklarının korozyonu, betonarme yapıların bozulmasının en önemli nedenlerinden biridir. Korozyona bağlı güvenlik sorunları ve mevcut yapıların onarımı için kullanılacak gerekli ve mevcut bütçeler arasındaki fark, rehabilitasyon projelerini doğru bir şekilde önceliklendirerek maliyetleri optimize etmek ve yapısal güvenlik sorunlarının üstesinden gelmek içinyapıların hizmet ömrünün güvenilir bir şekilde tahmin edilmesini oldukça kritik hale getirmektedir. Bu çalışmada, saha incelemeleri ile belirlenen mevcut korozyon seviyelerine göre mevcut yapıların gelecekteki korozyon yayılımını tahmin etmek için Reverse Monte Carlo yöntemi kullanılmıştır. Önerilen yöntemin yeniliği, gelecekteki korozyon yayılımına ilişkin beklentilerin güvenilirliğini artırmak için donatıların mevcut korozyon seviyelerini kullanmasıdır. Başka bir deyişle, saha ölçümleri, korozyon seviyelerini tahmin etmek için kullanılan matematiksel modellerin doğrulanabileceği referans noktaları olarak kullanılmaktadır. Yeni Zelanda'da bulunan ve 1928'de inşa edilen korozyona uğramış betonarme bir bina için önerilen yöntem kullanılarak bir vaka çalışması yapılmıştır. İlk adım olarak, binanın mevcut korozyon seviyesi, korozyonun gelecekte nasıl yayılabileceğini tahmin etmek için kullanılmıştır. Daha sonra OpenSees platformu kullanılarak binanın sonlu eleman modeli geliştirilmiş ve binanın gelecekteki sismik performansını değerlendirmek için doğrusal olmayan statik analizler gerçekleştirilmiştir. Sonuçlar, bir binanın mevcut korozyon seviyelerine ilişkin verilerin, mevcut binaların gelecekteki sismik performansları için güvenilir tahminler yapmak için değerli bir girdi olabileceğini göstermektedir.

TABLE OF CONTENTS

ACKNOWLEDGEMENTS iv
ABSTRACT v
ÖZET vi
LIST OF FIGURES ix
LIST OF TABLES xii
LIST OF SYMBOLS xiii
LIST OF ACRONYMS/ABBREVIATIONS xv
1. INTRODUCTION 1
1.1. Objective 1
1.2. Literature Review 4
1.2.1. Mechanical Properties of Corroded Reinforcement 4
1.2.2. Structural Performance of Corroded RC Elements 7
1.2.3. Numerical Modeling of Corroded RC Elements 10
1.2.4. Seismic Reliability Analysis of Corroded RC Structures 12
1.2.5. Building Stock and Regional Seismic Risk Assessment of Istanbul 16
1.2.6. Corrosion Monitoring 18
1.3. Thesis Outline 21
2. CORROSION OF REINFORCED CONCRETE STRUCTURES 22
2.1. General 22
2.2. Factors Affecting the Corrosion Process of Steel Bars in Concrete . . . 24
2.3. Diffusion Process 28
2.4. Corrosion Initiation Time 29
2.5. Effects of Corrosion on Reinforcing Bars 30
2.6. Effects of Corrosion on Unconfined Concrete 31
2.7. Effects of Corrosion on Confined Concrete 32
3. FUTURE CORROSION PROPAGATION 33
3.1. Monte Carlo Simulation 33
3.2. Reverse Monte Carlo 36

4. CASE-STUDY: TIME-DEPENDENT SEISMIC PERFORMANCE OF RC BUILDINGS 41
4.1. Building 41
4.2. Corrosion Propagation 43
4.3. Structural Modeling 49
4.3.1. OpenSees 49
4.3.2. Material Model of Reinforcing Bars 50
4.3.3. Material Model of Unconfined Concrete 51
4.3.4. Material Model of Confined Concrete 52
4.3.5. Modeling of Columns and Beams 55
4.4. Nonlinear Static Analysis 59
4.5. Time-Dependent Seismic Performance 67
5. CONCLUSION 72
6. REFERENCES 75

LIST OF FIGURES

Figure 2.1. Schematic demonstration of the corrosion of steel bar in concrete (Naidu Gopu and Joseph, 2022). 23

Figure 2.2. Stages of the reinforcement corrosion. 25

Figure 2.3. Effects of corrosion on reinforcement. 26

Figure 2.4. Effects of corrosion propagation on concrete. 26

Figure 2.5. Demonstration of effects of corrosion on concrete. 27

Figure 2.6. Cracking of cover concrete due to corrosion. 27

Figure 2.7. Concrete spalling due to corrosion. 28

Figure 3.1. RMC method to estimate future corrosion propagation. 39

Figure 3.2. Monte-Carlo simulation to predict today's corrosion level. 40

Figure 3.3. Future corrosion propagation using RMC. 40

Figure 4.1. Layout of the case study building: (a) plan; (b) elevation (Nataraj et.al 2021). 41

Figure 4.2. Cross-sections of the beams (Nataraj et.al 2021). 42

Figure 4.3. Cross-sections of the columns (Nataraj et.al 2021). 42

Figure 4.4. Condition assessment of the case study building (Nataraj et.al 2021). 43

Figure 4.5. Comparison of the distribution of corrosion levels. 45

Figure 4.6. Corrosion predictions for 10 years later. 46

Figure 4.7. Corrosion predictions for 20 years later. 47

Figure 4.8. Corrosion predictions for 30 years later. 47

Figure 4.9. Corrosion predictions for 40 years later. 48

Figure 4.10. Corrosion predictions for 50 years later. 48

Figure 4.11. Idealized beam-column models considering both concentrated and distributed plasticity (Astroza et.al. 2015). 56

Figure 4.12. Three-dimensional visualization of the OpenSees model. 58

Figure 4.13. Design spectrum vs capacity spectrum. 61

Figure 4.14. Drift ratios in the east-west direction: (a) 10 years later, (b) 20 years later, (c) 30 years later, (d) 40 years later, (e) 50 years later. 62

Figure 4.15. Drift ratios in the north-south direction: (a) 10 years later, (b) 20 years later, (c) 30 years later, (d) 40 years later, (e) 50 years later. 62

Figure 4.16. Stress-strain behavior of steel with 15% corrosion. 64

Figure 4.17. Stress-strain behavior of steel with 30% corrosion. 64

Figure 4.18. Stress-strain behavior of steel with 40% corrosion. 65

Figure 4.19. Stress-strain behavior of steel with 42% corrosion. 65

Figure 4.20. Distribution of the maximum drift ratios (east-west direction). . . 66

Figure 4.21. Distribution of the maximum drift ratios (north-south direction). . 67

Figure 4.22. Cumulative distribution of the maximum drift ratio in east-west direction. 68

Figure 4.23. Cumulative distribution of the maximum drift ratio in north-south direction. 69

Figure 4.24. Time-variant failure probability of building. 70

LIST OF TABLES

Table 1.1. Age distribution of building stock in Istanbul (Konukcu et.al 2017). 1

Table 2.1. Random variables. 29

Table 4.1. Summary of the RMC process. 44

Table 4.2. Skewness and kurtosis of distributions. 45

Table 4.3. Material properties - concrete. 54

Table 4.4. Material properties - steel. 54

Table 4.5. Change in ductility levels of core concrete. 55

Table 4.6. Natural periods of the building in EW direction. 60

Table 4.7. Limit state threshold values for inter-story drift ratios. 69

Table 4.8. Time-variant failure probabilities (Collapse Prevention). 70

LIST OF SYMBOLS

a	Aging coefficient
A_0	Initial net cross-sectional area of reinforcement
A_{cor}	Cross-sectional area of the corroded reinforcement
b_0	Original width of the cross section
b_1	Increased width due to corrosion cracks
c	Concrete cover (mm)
c_0	Initial chloride content in the cement paste
C_{crit}	Critical chloride content (wt. % concrete)
C^p	Corrosion levels predicted via diffusion process model
C^t	Existing corrosion levels determined via site inspections
$C_{s,\Delta x}$	Chloride content (wt. % concrete)
D_{RCM}	Chloride migration coefficient (m^2/sec)
$D_{app,c(t)}$	Apparent coefficient of chloride diffusion
f_{cc}	Compressive strength of concrete
M_0	Mass of non-corroded reinforcement
M_{corr}	Mass of the corroded reinforcement
Q_{corr}	Corrosion level (%) of reinforcement
R	Coefficient of roughness and diameter of reinforcement
t_{28}	Reference initial time (28 days)
V	Volumetric expansion ratio of the corrosion products
w	Total crack width
w_i	Width of the $\mathrm{i}^{th} crack$
x_b	Corrosion level
X_0	Error
Δx	Depth of the convection zone
ϵ_a	Average tensile strain in the cracked concrete
ϵ_c	Compressive strain of confined concrete

ϵ_{co}	Concrete strain at the compressive strain $\sigma_c^{'}$
ϵ_{coc}	Ultimate compressive strain of concrete
ϵ_u	Ultimate strain of the corroded reinforcement
ϵ_{uo}	Ultimate strain of non-corroded reinforcement
σ	Test error
σ_c	Compressive stress of confined concrete
$\sigma_c^{'}$	Compressive strength of cover concrete w/o corrosion
σ_c^r	Reduced compressive strength of cover concrete w/ corrosion
σ_y	Yield strength of non-corroded reinforcement
$\sigma_y^{'}$	Yield strength of the corroded reinforcement

LIST OF ACRONYMS/ABBREVIATIONS

3D	Three Dimensional
ASTM	American Society for Testing and Materials
CALTRANS	California Department of Transportation
CBECS	Commercial Buildings Energy Consumption Survey
CT	Computed Tomography
FEMA	Federal Emergency Management Agency
NACE	National Association of Corrosion Engineers
RC	Reinforced Concrete
RMC	Reverse Monte Carlo
TDBY	Turkish Seismic Design Code

1. INTRODUCTION

1.1. Objective

A significant number of existing buildings are older than 50 years and a remarkable portion of these structures is located in seismically active regions such as Greece, Italy, Japan, New Zealand, Turkey and United States (CBECS Survey Data 2018; Filippidou & Navarro 2019; Economidou 2011). For instance, construction dates and age distribution of buildings located in Istanbul is presented in Table 1.1 (Konukcu et.al 2017). Therefore, to make reliable seismic performance estimations for existing buildings is an inevitable pre-requisite to develop effective strategies to improve the resilience of societies against the earthquake events.

Table 1.1. Age distribution of building stock in Istanbul (Konukcu et.al 2017).

Constructin Date	**Approx. Age**	**Building Numbers**	**Percentage**
Pre-1968	t>50	82.828	8.36%
Between 1969-1982	40<t<50	330.489	33.36%
Between 1983-1996	30<t<40	381.008	38.46%
Between 1997-2004	20<t<30	114.480	11.56%
Between 2005-2007	10<t<20	46.336	4.68%
Between 2008-2013	t<10	35.443	3.58%

On the other hand, estimation of the structural performance under seismic excitation is a challenging task due to uncertainties in the seismic demands and the structural capacity to withstand these demands against damage and collapse. It is common in seismic risk estimation to group these uncertainties into two categories which represent the uncertainties stem from factors that are inherently random (aleatoric uncertainty) and uncertainty due to lack of knowledge or ignorance (epistemic uncertainty) (Wen et.al, 2003). The aleatoric uncertainty can be classified as variation in ground motion properties such as the exact location, magnitude and time of future earthquake events. On the other hand, spatial distribution of potential seismic zones, the predicted maximum earthquake magnitude, and the recurrence periods for earthquakes of different magnitudes are continuously being investigated and new models are being developed and updated based on the current and new knowledge to reduce the epistemic part of the uncertainty in future earthquakes.

Epistemic uncertainties in structural capacity estimation are mainly originated from the variation in material and geometric properties (Tyagunov et al. 2014, Choudhury & Kaushik, 2019). In addition to variations in the as-built material properties, time-dependent changes in materials due to environmental effects can also be considered as important sources of epistemic uncertainties in structural capacity predictions. Degradation of reinforcing bars due to corrosion under chloride attacks can be one of the main reasons of the deterioration of reinforced concrete structures and it can cause changes in both material and geometric properties such as the reduction of cross sections of reinforcing bars, degradation of the bonds between concrete and reinforcing bars, and cracking of concrete (Apostopoulos & Papadakis 2008; Pape & Melchers 2010; Fernandez et.al 2018; Ou et.al 2016; Vanama & Ramakrishan 2020). Moreover, insufficient performance of corroded reinforcing concrete buildings has been observed during the field inspections after several earthquakes (Kaushik & Jain 2007; Sharma et.al 2016; Freddi et.al 2021). Therefore, it became inevitable to consider the corrosion and earthquake hazards simultaneously in order to make reliable seismic performance estimations for existing buildings.

Numerous experimental studies have been carried out to identify the effects of corrosion on material properties of corroded reinforcing bars and structural elements (Zhang et.al 1995; Dhakal & Maekawa 2002; Du et.al 2005; Apostolopoulos & Michalopoulos 2006; Kashani et.al 2013; Fernandez et.al 2015; Kashani et.al 2015; Ou et.al 2016; Meda et.al 2014; Guo et.al 2015; Kashani et.al 2016; Yuan et.al 2017; Rajput & Sharma 2018; Yuan et.al 2017; Vu & Li 2018). In addition, various analytical models have been developed in order to estimate the seismic performance of existing reinforced concrete buildings exposed to corrosion (Kashani et.al 2015; Fernandez et.al 2016; Bru et.al 2018; Imperatore & Rinaldi 2019; Di Sarno & Pugliese 2020). The results of these studies are valuable inputs for finite element models to eliminate the material and geometric uncertainties originated from the corroded reinforcements.

Changes in structural capacity and seismic reliability of corroded RC structures are other topics that have been intensively investigated (Alipour et.al 2011; Zanini et al. 2013; Alipour et.al 2013; Biondini et.al 2014; Biondini et.al 2015; Goksu & Ilki 2016; Goksu et.al 2016; Cui et al. 2018; Ghosh & Padgett 2010; Guo et al. 2015; Rao et.al 2016; Titi et al., 2018; Zanini et.al 2017; Hasanzadeh et.al 2021; Lejouad et.al 2022). The main purposes of these studies are, first to obtain the remaining structural capacities of corroded RC structures via experiments or analytical analyses and second to predict the seismic reliability for expected earthquake events. Since the seismic reliability estimations of existing buildings are sensitive to the corrosion levels of the structural elements, the importance of site inspections and long-term corrosion monitoring have been gradually increasing. Most of the corrosion data available in the literature have been obtained from the reinforcements corroded in the laboratory environment. Therefore, recent inspection and monitoring activities are quite valuable for not only to measure the existing corrosion levels of the reinforcements but also to identify the mechanical properties of naturally corroded reinforcements better and to improve the numerical models used to predict future corrosion propagation (Totani et.al 2021, Li et.al 2022 and Li et.al 2022).

Although various aspects of the corrosion have been studied, there is still a lack of information about the relation between the existing corrosion levels and the long-term seismic performance estimation of reinforced concrete buildings. Therefore, the purpose of this study is to present a methodology that can be used to reliably predict the future corrosion propagation in a structure. The contribution of the proposed methodology to the field is to use existing corrosion levels identified by site inspections to make predictions for the future corrosion propagation. In other words, it utilizes the experimental measurements as references in order to decrease the effects of epistemic uncertainties in the numerical models of corrosion propagation. As a result, the validated corrosion models can be used to make more reliable estimations for the future corrosion levels and structural performance under earthquake excitations can be assessed accordingly.

1.2. Literature Review

1.2.1. Mechanical Properties of Corroded Reinforcement

Effects of corrosion on the mechanical properties of reinforcing bars have been widely studied by researchers. The main focus of these studies is to identify the changes in the strength, strain capacity and cross-sectional area of the corroded steel bars. Since it cannot always be possible to collect samples from existing structures, some of the laboratory tests have been conducted using the artificially corroded reinforcing bars.

Almusallam (2001) carried out a study to identify the effects of corrosion on the mechanical properties of steel longitudinal bars. Accelerated corrosion process was applied to the reinforced concrete elements and the corroded reinforcements were removed afterwards to conduct laboratory tests. In order to investigate the effect of initial diameter of reinforcements on the change in mechanical properties, two diameters, which were 6 mm and 12 mm, were considered for the specimens. Significant reductions in both tensile strength and deformation capacity of steel bars were noted according to test results.

Du et.al. (2005) presented the results of an experimental investigation on ductility of reinforcing bars exposed to corrosion. Artificial corrosion process was applied to both bare reinforcements and steel bars embedded into concrete. In total, 108 specimens, consisting of 18 uncorroded and 84 corroded bars, were tested until the rupture of reinforcements in order to measure the strength and ductility behavior. They observed notable reductions of strength and ductility capacities of the steel reinforcement subjected to corrosion. Moreover, regression analyses were carried out to identify the relation between change in corrosion levels and mechanical properties. Finally, researchers developed equations in accordance with the results of regression analyses.

Zhang et.al. (2012) conducted an experimental study to investigate the effects of corrosion on the tensile and fatigue behavior of longitudinal reinforcements. Accelerated corrosion process was utilized by researchers in order to obtain artificially corroded specimens in addition to the naturally corroded steel bars taken from a 30-year-old building. According to the tensile test result, they reported significant reduction in the strength capacities due to corrosion and they stated that decrease in the ultimate strength was more critical than the reduction of yield strength. Additionally, they observed severe reduction in the deformability capacities of reinforcements due to adverse impacts of corrosion. Furthermore, researchers observed a remarkable decrease in the fatigue life of steel reinforcements, and they also reported that the fatigue behavior of reinforcing bars was affected more when compared with the tensile behavior.

Kashani et.al. (2013) investigated the adverse impacts of corrosion on the nonlinear cyclic behavior of steel reinforcements. For this purpose, they prepared 39 specimens with various corrosion levels and slenderness ratios. They reported that cyclic behavior of reinforcing bars was significantly affected by the mass loss due to corrosion. Since the slenderness ratio of a reinforced concrete element will be increased due to corrosion of lateral reinforcements, the degradation of low-cycle fatigue behavior of longitudinal reinforcements due inelastic buckling of corroded bars should be taken into consideration when conducting a seismic performance evaluation.

Fernandez et.al. (2015) carried out an experimental study to investigate the effects of corrosion on the mechanical properties of steel reinforcements. For this purpose, 180 artificially corroded specimens were tested. Researchers performed 40 monotonic tests as well as 140 fatigue tests. They reported strong correlation between corrosion levels of the steel bars and degradation of the mechanical properties such as yield and ultimate stress, modulus of elasticity and fatigue life.

Ou et.al. (2016) examined the influence of corrosion on the tensile behavior of longitudinal reinforcing bars. For this purpose, 18 corroded reinforcing bars were obtained from a residential building constructed in the 1970s and located in a marine area. Additionally, they performed an accelerated corrosion process for the 29 specimens to get the artificially corroded steel reinforcements. Researchers tested both naturally and artificially corroded reinforcing bars under tensile loadings. They reported that strength and deformation capacities of reinforcements were significantly reduced due to adverse effects of corrosion. Furthermore, different reduction factors were proposed by researchers to reflect the impacts of natural and artificial corrosions on the tensile behavior of steel reinforcements separately.

Imperatore et.al. (2017) carried out an experimental survey on the steel reinforcing bars with different diameters and varying corrosion levels in order to observe the relation between corrosion and deterioration of mechanical properties. In total, 35 specimens were subjected to accelerated corrosion process in the laboratory environment, and they were applied monotonic loadings to investigate the change in tensile behavior. Strength and strain data measured during the tensile tests were converted to a non-dimensional form to make linear and exponential regression analyses. As a result, they proposed reduction factors for the yield and ultimate strengths and ultimate strain of reinforcement, which are functions of mechanical properties of uncorroded steel bars and the corrosion levels.

Vanama and Ramakrishnan (2020) conducted a comprehensive experimental study on the mechanical properties of 38 naturally corroded and 15 artificially corroded reinforcing bars. Naturally corroded steel bars were extracted from a 54-year-old building. The results show that yield and ultimate stress values and ductility of both naturally and artificially corroded reinforcements reduced significantly. Although naturally and artificially corroded bars present similar global behaviors, decrease in stress and strain levels is higher for naturally corroded reinforcements than the artificially corroded ones.

1.2.2. Structural Performance of Corroded RC Elements

Although the information obtained by the experiments on corroded steel bars are valuable from the structural engineering point of view, to determine the influence of changes in the mechanical properties of reinforcements to the overall performance of RC structural elements are also valuable for several purposes. First of all, ductility limits of the RC elements exposed to corrosion is valuable to be able to determine the changes in the performance limits such as drift ratios or rotations. In addition, the results of structural element tests can be used as the reference behavior according to which the numerical models simulating the corroded RC elements can be validated. Moreover, it is crucial to observe whether various assumptions are still valid for the RC elements exposed to corrosion.

Meda et.al. (2014) evaluated the structural performance of reinforced concrete columns under cyclic loads. For this purpose, authors used four specimens. Reinforcements of the two columns were extracted from the specimens and tested in tension, in order to determine the effect of the concrete presence during the corrosion process. One of the other specimens was corroded and used in the cyclic test in order to observe the effect of corrosion on the cyclic performance whereas remaining specimen was the uncorroded reference one that was also tested to obtain the seismic behavior of RC columns without the influence of corrosion. Decreases in the yield and ultimate strengths and in the ultimate strain were identified in corroded steel bars. Researchers also stated that the global seismic behavior of RC columns was also significantly affected by the corrosion. They observed almost 30% decrease in the ultimate force and a reduction of ultimate displacement of about 50% in addition to a significant decrease in the stiffness during the last cycles.

Goksu and Ilki (2016) carried out an experimental study to determine the structural behavior of corroded reinforced concrete columns under reverse cyclic loads. They used six artificially corroded specimens with varying corrosion levels from 0% to 54%. Researchers reported that columns mainly failed due the fracture of the corroded reinforcements and as a result the drift ratio decreased from 8% to 2% from uncorroded bars to severely corroded reinforcements. Reduction of drift ration caused significant decrease in the energy dissipation capacities of corroded columns.

Ou and Nguyen (2016) conducted laboratory tests on the corroded reinforced concrete beams in order to investigate the effect of location of reinforcement corrosion on seismic performance of beams. Artificial corrosion method was induced to beams in order to develop corroded reinforcement at various locations of the specimens. Researchers reported that for beams the effects of corrosion of longitudinal tension bars has significant negative impacts on the yield and peak loads as well as yield and ultimate drift capacities whereas corrosion in the compression bars has very limited effects. Corrosion in the transverse bars can also negatively affect the yield and ultimate drift capacities of the reinforced concrete beams but it has insignificant influence on the yield and ultimate loads.

Liu et.al. (2017) conducted an experimental study using six reinforced concrete moment-resisting frames in order to examine the influence of corroded longitudinal reinforcing bars on the structural performance of reinforced concrete frames under cyclic loadings. Five of the specimens were corroded whereas the remaining frame was uncorroded and used as the reference one. Researchers reported that increased corrosion level caused the reduction of lateral load carrying capacity, deformation capacity as well as the energy dissipation capacity of the reinforced concrete frames.

Yuan et.al. (2017) tested six circular RC bridge piers with different corrosion levels under cyclic loading. One specimen was considered as the sound structural element and not exposed to artificial corrosion process. On the other hand, five specimens were subjected to accelerated corrosion process with durations of 30, 60, 105, 130 and 150 days in order to obtain varying corrosion levels. The most interesting result presented by the researchers is that the difference in the cyclic behavior of the corroded and uncorroded RC piers was not critical when the corrosion level is around 8-9% whereas there were significant decreases in the strength, energy dissipation and deformation capabilities of the bridge piers with corrosion levels larger than 17%.

Yuan et.al. (2017) carried out experimental study using the eight reinforced concrete columns, seven of which were exposed to accelerated corrosion in the laboratory environment whereas one of the specimens was used as the reference uncorroded sample. Corrosion levels of the longitudinal bars of the artificially corroded specimens varied from 3.83% to 8.41%. Repeated axial loads were applied to four corroded specimens before the low cycle reversed loads. They observed that corrosion of the reinforcing bars had a significant effect on the yield strength and ultimate load bearing capacity under cyclic loading. Although they applied repeated axial load to four corroded columns before the cyclic horizontal loading to simulate the vertical pounding, they did not report any crucial influence of these loadings on the yield strength and load bearing capacity of reinforced concrete columns exposed to corrosion.

Rajput & Sharma (2018) conducted experiments on the six reinforced concrete columns in order to investigate the impacts of corrosion for seismic performance of columns casted according to modern seismic codes and guidelines. They divided the reinforced concrete columns into two categories as experiment and control groups. The former one consisted of three reinforced concrete columns which were artificially corroded up to 15% of corrosion level whereas the latter category included the uncorroded specimens. The first result stated by the authors is the significant decrease in the cross-sectional area of the steel bars due to increasing corrosion level. The decreased cross-sectional areas of the reinforcements caused the reduced ductility capacities of the columns due to losing the effective confinement. Furthermore, they also mentioned that catastrophic failures had also occurred due to significant reduction in the load carrying capacity.

Vu and Li (2018) conducted an experimental study using the eight columns consisted of both uncorroded and corroded specimens which were applied quasi-static cyclic loading. They reported that corrosion of the reinforcing bars significantly affects the seismic behavior such as lateral load capacity, yield displacement, ductility capacity, hysteretic response, energy dissipation capacity and cracking pattern.

Yuan et.al (2018) presented the results of shaking table tests carried out for four reinforced concrete bridge piers with different degrees of corrosion. They applied a series of increasing ground motions to the bridge piers and measured and analyzed the displacement response, natural periods, damping ratios, acceleration response and curvature distribution of the specimens. They reported increased natural period and higher damping ratio with increased level of corrosion.

1.2.3. Numerical Modeling of Corroded RC Elements

The primary objective of research studies focusing on the corroded reinforcements or RC elements exposed to corrosion attacks is to provide useful inputs to the remaining capacity estimations and reliability analyses. For this purpose, the information obtained via the laboratory tests must be transformed to numerical models that can be used for the finite element analyses of the RC structures. Various models focusing on the different aspects such as ductility, buckling, cyclic behavior etc. have been proposed by other researchers.

Goksu et.al (2015) developed a bond-slip model in order to simulate the bond characteristics between concrete and reinforcing bars. The novelty of this study is that researchers considered the concrete with low compressive strength and plain reinforcements, which are typical construction materials of the majority of existing reinforced concrete buildings. The proposed model account for the reversed cyclic lateral loading tests of full-scale substandard RC columns. The main contribution of this new model is to predict the changes in bond strength in accordance with the corrosion levels of the reinforcing bars. They used the experimental results available in the literature in order to verify the estimations of the proposed model.

Kashani et.al (2015) developed a hysteretic numerical model for steel reinforcements with and without corrosion effects. The model can represent the buckling of reinforcing bars, deterioration in compressive strength due to post-buckling strain records and tension behavior affected by low-cycle high-amplitude fatigue. They used the response history of both uncorroded and corroded reinforcing bars obtained from laboratory experiments in order to verify the effectiveness of the proposed model in simulation of hysteretic behavior of uncorroded and corroded bars.

Fernandez et.al (2016) proposed a mechanical model in order to simulate stress – strain behavior and fatigue curves of corroded reinforcing bars. They take into account both generalized corrosion and pitting corrosion when developing the model. In order to calibrate the proposed model, researchers used experimental results obtained from both monotonic and cyclic tests of corroded reinforcing bars.

Kashani et.al (2016) proposed a modelling technique via OpenSees and it simulates the effect of corrosion on mechanical properties of steel bars such as buckling, pitting, decreased low-cycle fatigue life and ductility loss, cracked concrete cover and reduction of ductility and capacity of the core concrete. Researchers utilizes the Dhakal-Maekawa model in order to represent the buckling behavior of corroded reinforcements, but the novelty of the study is that researchers used this model for a circular column and compare the numerical simulation results with the responses measured from a laboratory test of corroded circular RC column. Afterwards, they carried out the pushover analyses for mentioned column considering the different corrosion scenarios. The results shows that both lateral load-carrying and the ductility capacities of the reinforced concrete columns decrease significantly with the increasing corrosion levels.

Qiu and Gong (2019) proposed a numerical model for the hysteretic behavior of steel reinforcements taking into account the impact of inelastic buckling and low-cycle fatigue. They presented a formula, which is in the Bouc-Wen model, for the post-yield stiffness ratio depending on the strain value. In addition, they utilized the Genetic Algorithm to determine model control parameters in accordance with the hysteretic loops of steel reinforcements obtained by laboratory experiments. The effectiveness of presented model was verified by comparing the numerical analyses results with the experimental ones for both reinforced concrete columns and reinforcing bars.

Imperatore and Rinaldi (2019) conducted a comprehensive experimental study in order to identify the effects of corrosion on the buckling behavior of corroded reinforcing bars. The scope of the experiment included specimens with various slenderness ratios and different corrosion levels. The results of this experimental program showed that corrosion level significantly affects the stress capacity of the reinforcements under compression as well as their post-buckling behavior. Therefore, researchers developed an analytical model to estimate these mechanical properties of the corroded longitudinal reinforcements.

1.2.4. Seismic Reliability Analysis of Corroded RC Structures

Decision-makers need to obtain reliable information about the seismic performance estimations of existing structures in order to use the limited resources effectively. The governing question that must be answered in this regard is the long-term effects of the capacity reduction due to corrosion on the seismic performance of RC structures. For this purpose, various probabilistic methodologies have been proposed and several case studies have been presented by other researchers.

Ghosh and Padgett (2010) presented a framework to determine the time-dependent fragility curves of reinforced concrete bridges exposed to corrosion. They developed a finite element model of the bridge on the OpenSees platform and utilized a probabilistic approach in order to capture the effects of corrosion on the reinforcements. They considered only the reduction of the cross-sectional area of the longitudinal reinforcements although the effects of corrosion on the yield strength and strain capacities of steel bars have been reported by other researchers. They reported significant reduction in both load-carrying capacity and ductility of the reinforced concrete bridge columns. As a result, they presented the results of the fragility analyses carried out for different ages of the bridge, showing a significant increase in the failure probability for different damage states.

Alipour et.al (2011) showed a numerical study carried out to estimate the lifetime structural performance and life-cycle cost of reinforced concrete bridges exposed to corrosion and located on the seismically active zones. First of all, they determined the corrosion initiation time for the bridges in accordance with the chloride diffusion equation and then the extent of the structural deterioration was estimated over the entire life of the bridge. Time-dependent fragility curves were generated by the researchers to conduct a probabilistic seismic risk assessment.

Alipour et.al. (2013) proposed a procedure to evaluate the structural performance as well as the life-cycle costs of reinforced concrete bridges exposed to chloride attacks. They estimate the effects of chloride diffusion on the geometrical and material properties of the structural elements over the life-time period of a bridge. The capacity loss of the bridges was evaluated using the moment-curvature and pushover analyses. In order to determine the optimum life-cycle costs, researchers proposed maintenance and inspection intervals according to predicted reduction of load carrying capacities due to corrosion of reinforcing bars.

Inci et.al. (2013) presented the numerical analyses of reinforced concrete frame buildings in order to show the unfavorable impacts of the corrosion on the structural performance. For this purpose, both nonlinear static analysis and nonlinear time-history analysis were carried out for ten hypothetical buildings considering various corrosion levels and different earthquake records. They reported that the reduction of cross-sectional area of the steel bars and the decrease in the displacement capacity of structural elements or buildings are the most significant adverse effects of the corrosion.

Biondini et.al (2013) presented life-cycle seismic performance reinforced concrete bridges exposed to corrosion. They followed a probabilistic approach in order to consider the uncertainties involved in the chloride-induced diffusion process as well as the geometrical and material properties of structural elements. A four-span reinforced concrete bridge was analyzed by the researchers to present the application of proposed procedure. The results of this study showed that the base shear capacity, ductility and yield and ultimate displacements decrease significantly through the lifetime of a reinforced concrete structures.

Zanini et.al (2013) examined the maintenance management and planning of bridge networks located in seismically active areas considering the deterioration of the structural elements due to chloride-attacks. In order evaluate the seismic performance of bridges, they developed the ductility-based fragility curves for which the effects of corrosion were modelled as decrease in the cross-sectional area and yield strength of reinforcing bars. Afterwards, they evaluate the effects of retrofitting on the seismic performance of bridges. For this purpose, they presented three different retrofitting approaches which were numerically applied to 60 years old bridge. Accordingly, the seismic vulnerabilities of bridge with and without retrofitting were calculated to predict the changes in seismic performance. As expected, the seismic performance of the bridge, especially in the weak direction, was significantly improved after retrofitting.

Biondini et.al (2015) presented a probabilistic framework to life-cycle assessment of seismic resilience of aging reinforced concrete structures. They considered the adverse effects of aggressive environmental conditions such as chloride diffusion on the structural members in order to identify the role of deterioration on the recovery process after an earthquake event. The results of the case studies showed that due to adverse effects of corrosion on the structural performance of reinforced concrete members, both load-carrying capacity, for instance base-shear, and the displacement ductility were significantly reduced. They stated that the one of the reasons of significant decrease in load-carrying capacity could be the change in plastic hinge locations which might lead to the activation of collapse mechanisms with lower ductility and energy dissipation capacity.

Guo et.al (2015) examined the time-dependent seismic performance assessment of coastal bridges under the adverse impacts of chloride attacks. For this purpose, they integrate the traditional fragility curve analysis with the structural deterioration inputs due to corrosion of reinforcing bars. In order to investigate the effects of depth of cover concrete on the corrosion initiation time, they also carried out a sensitivity analysis considering three different depths. Furthermore, they aimed to identify the corrosion propagation on reinforcement bars located at the different zones on a column, which were named as atmospheric zone at the top one third of the column and splash and tidal zone at the middle of a column. Similar to other researchers, they reported a significant decrease in the load-carrying capacity and ductility of columns and dramatic increase in the failure probability of reinforced concrete bridges due to negative effects of corrosion.

Rao et.al (2016) proposed a model to calculate the fragility functions which depend on the structural deterioration level. The model account for the changes in structural capacity and demand due to corrosion of steel bars. The effects of the structural deterioration were modelled by reduction of the cross-sectional area of the steel bars, strength of the cover concrete and the bond strength. They considered the damage states proposed by the CALTRANS to develop the fragility functions of the reinforced concrete columns exposed to corrosion. Afterwards, failure probabilities were calculated considering the different corrosion levels and the results showed a significant increase in the failure probabilities with increased level of corrosion.

Zanini et.al (2017) proposed a time-dependent probabilistic seismic risk forecasting framework for bridge networks. In order to have a fully time-dependent assessment procedure, they considered not only the deterioration of the structure due to environmental effects such as corrosion, but also the time-value of the money which might be used for retrofitting or reconstruction of the bridges. They applied the presented time-dependent risk assessment framework to a network located North-East Italy and consisted of 500 bridges and compared the results of the proposed procedure with the ones obtained by traditional seismic risk assessment methods. They reported significant differences between average annual losses predicted via traditional fragility analyses and the proposed forecasting framework.

Titi et.al (2018) examined the lifetime structural performance of reinforced concrete frames exposed to corrosion. In order to take into account the uncertainties related to chloride attacks, materials and modeling assumptions, they utilized Monte Carlo Simulation. The procedure proposed by the study was applied to a three-storey reinforced concrete frame and seismic performance of the structure was investigated pushover analysis. The results revealed that due to increased level of corrosion, both load-carrying capacity and ductility of the reinforced concrete frames decrease significantly.

Li et.al. (2022) proposed a framework to evaluate the time-dependent seismic performance reinforced concrete highway bridges considering the environmental effects such as chloride attacks. Degradation in mechanical properties were modeled as the changes in yield strength and cross-sectional area of the reinforcing bars and compressive strength of the core concrete. They applied the proposed framework to a highway bridge. The results showed that the moment and ductility capacities of the reinforced concrete columns decreased significantly with increased level of corrosion. As a result, failure probabilities of bridges increased dramatically especially for the extensive and collapse damage states.

1.2.5. Building Stock and Regional Seismic Risk Assessment of Istanbul

Sucuoğlu et.al (2007) proposed a procedure for the seismic risk assessment of existing building stocks. To collect data from each and every building cannot be possible due to time and resource limitations, therefore researchers proposed a systematic sidewalk survey in order to collect visual data in order to classify the buildings into expected performance levels. The parameters considered to classification obtained via this survey are having a soft story or not, construction quality that is apparent from the outside and having overhangs or not. Nowadays, with new technologies, it would be possible to conduct this survey faster via cars and high resolution cameras and the categorization may be performed via image processing tools.

Yakut et.al (2007) presented the application of a seismic risk prioritization approach to the residential buildings located in Istanbul. The main parameters for the seismic performance of existing buildings can be identified during a systematic sidewalk survey and the method can be applied to mid-rise buildings. They performed the proposed method to 100.000 buildings and they reported that 52% of the building as high-risk in terms of seismic performance. In other words, for 52.000 buildings studied by the researchers, the expected seismic damages are either severe damage or collapse.

Bal et.al (2008) proposed a Displacement-Based Earthquake Loss Assessment methodology for existing building stock. In the proposed procedure, building stock is modeled as a random population of building classes with taking into account the distributions of geometrical and material properties. Building height and type are used in order to estimate the natural periods of the buildings, which is important to calculate the displacement demand for each building separately. On the other hand, displacement capacity of each building is obtained utilizing the variations in the geometrical and material properties. Finally, the displacement demand and capacity are compared with each other in order to predict the seismic performance of buildings.

The period of vibration of each building in the random population is calculated using a simplified equation based on the height of the building and building type, while the displacement capacity at different limit states is predicted using simple equations which are a function of the randomly simulated geometrical and material properties.

Strasser et.al (2008) conducted a numerical study in order to compare the loss estimations that can be obtained utilizing various Earthquake Loss Estimation methodologies. Seismic damage predictions were performed for the building stock in Istanbul via software packages KOERILOSS, SELENA, ESCENARIS, SIGE, and DBELA. They reported that the spatial distributions of damage predicted by different packages are similar not only to each other but also to estimations made for Istanbul by previous research studies.

Konukcu et.al (2017) presented a damage analysis for existing building stock of Istanbul. For this purpose, they utilized the building data available as of 2013. In order to carry out a regional seismic vulnerability assessment they considered the age of the buildings, floor numbers and type of construction as the governing parameters for the seismic performance of existing buildings. A software called HAZTURK was utilized by the researchers in order to perform the damage analysis for the building stock. They reported catastrophic consequences due to the insufficient seismic performance of old buildings due to both improper design and construction parameters and deterioration of buildings.

1.2.6. Corrosion Monitoring

The contributions of the structural monitoring on the reliable seismic performance estimations have been verified by various research studies. Since the corrosion is one of the most crucial parameters that can result in significant degradation in structural capacity, to determine the existing corrosion levels of the reinforcing bars is vital in order to achieve meaningful predictions. Therefore, there has been an increasing trend in the number of studies that focus on the site inspection or long-term corrosion monitoring. Some of these studies aim to propose new methods or tools that can be utilized in the corrosion monitoring practices whereas others intend to present the real-life applications.

Apostolopoulos and Papadakis (2008) carried out an experimental study in order to investigate the effects of corrosion on the ductility properties of steel reinforcements. They assessed the validity of the results obtained from steel bars corroded via artificial methods via specimens embedded in real-life structures and exposed to natural corrosion process. For this purpose, they used the reinforcement specimens from a 40-years old house located at the coastal area and a 30-years old industrial building. In order to determine the corrosion levels, they calculated the weight loss of specimens after removal of the rust by bristle brush method carried out according to ASTM specifications.

Patil et.al. (2017) conducted a non-destructive testing for two in-service reinforced concrete slabs in order to investigate the efficiency of acoustic emission methods for on-site corrosion prediction. The tested slabs were selected from different buildings and determined according to visual inspection results. One of the slabs were representing the undamaged structure whereas the other one used to represent the damaged due to corrosion. Two slabs were monitored via acoustic emission method continuously through 15 days to have reliable assessments for existing conditions. In addition to acoustic emission method, the test specimens were also assessed via half-cell potential technique to validate the results obtained by acoustic emission. They reported that continuous monitoring for a short period of time can provide proper data to evaluate the existing corrosion levels of reinforced concrete structures.

Fernandez et.al. (2018) investigated the reliability of corrosion levels determined by different cleaning methods as well as non-destructive testing approaches. The specimens were taken from a 30-years old bridge located in Sweden. Sandblasting, metallic brush and acid were chosen as the cleaning methods and 3D scanning and CT scanning were used as the non-destructive testing methods. For the cleaning methods, researchers reported the number of cleaning cycles should be ranged between 4 to 7 cycles in order to reach a difference in weight loss measurements lower than %0.2. In addition, they stated the sandblasting as the most reliable and effective method in corrosion removal. For the non-destructive testing methods, they found that results obtained by 3D scanning were very reliable whereas the CT scanning did not result in corrosion levels with high accuracy.

Van Steen et.al. (2019) carried out an experimental study to verify the corrosion levels identified by acoustic emission technique. For this purpose, small-scale reinforced concrete specimens built in the laboratory environment were exposed to artificial corrosion process. During the accelerated corrosion process, the specimens were monitored via acoustic emission method in order to determine the corrosion levels reliably. At an intermediate stage of the accelerated corrosion, they obtained the X-ray images of the specimens too. Researchers concluded that acoustic emission monitoring technique is sufficient to detect the corrosion levels for small-scale specimens and they noted a need for large-scale experiments for further verifications.

Fernandez and Berrocal (2019) examined the mechanical properties of corroded reinforcements extracted from a 30-years old bridge. They used the 3D laser scanning technique as the measurement tool for the cross-section of the reinforcing bars and they determine the variation of the corrosion levels along the reinforcement. In addition, cleaning of the bar was performed according to ASTM recommendation to measure the weight loss which is a most-commonly used parameter to determine the corrosion level.

Zheng et.al. (2020) carried out an experimental study on the reinforced concrete piles in a simulated marine environment condition in order to determine the efficiency of acoustic emission method on the corrosion monitoring and detection of localized corrosion. For this purpose, six large-scale reinforced concrete piles were subjected to accelerated corrosion and caused to have localized corrosion. During this process, two corroded and one uncorroded, reference, piles were continuously monitored using acoustic emission sensors. They stated that early detection of the microcrack initiation is possible via the conjunction analysis of several acoustic emission parameters. It is also reported by researchers that all acoustic emission sensors can detect the microcracking occurred at a distance of 0.4 m to 1.2 m.

1.3. Thesis Outline

In the first chapter, a literature review regarding effects of corrosion on the mechanical properties of steel reinforcements and structural performance of reinforced concrete elements, numerical modelling and seismic reliability assessment or reinforced concrete elements and structures and recent developments in corrosion monitoring is presented. Furthermore, the scope and the objectives of work has been denoted.

Chapter 2 can be considered as the corrosion chapter of this thesis. In this part, overview of the corrosion process of steel bars embedded in concrete is presented. In addition, effects of corrosion on reinforcements, unconfined concrete and core concrete are presented. Finally, numerical models used to simulate both diffusion process for concrete structures and the changes in material properties of steel and concrete are introduced.

The main motivation of Chapter 3 is to present the Reverse Monte Carlo method. For this purpose, first the applications of standard Monte Carlo Simulation in structural engineering are shown. Afterwards, the examples from applications of Reverse Monte Carlo in other fields are presented and the proposed methodology to estimate future corrosion propagation for reinforced concrete structures is introduced.

In the Chapter 4, the application of the proposed methodology is presented step-by-step via a Case Study. First of all, properties of the case study building and the results of the site inspections are presented. Afterwards, Reverse Monte Carlo method is performed to estimate the future corrosion propagation. According to design drawings and corrosion predictions, finite element model of the building is developed. Finally, nonlinear static analysis results and the time-dependent seismic performance estimations are presented.

Conclusions are presented in the last chapter.

2. CORROSION OF REINFORCED CONCRETE STRUCTURES

2.1. General

Corrosion can be defined as the deterioration of a metal due to a chemical or electrochemical reaction with its environment (NACE/ASTM G193). The surface of corroding reinforcement operates as the composite of cathodes and anodes electrically connected by the reinforcement itself, at which point coupled anodic and cathodic reactions occur (Ahmad, 2003). Reactions occurred at the anodes and cathodes are generally mentioned as half-cell reactions. Figure 2.1 presents the schematic illustration of the reinforcement corrosion in concrete.

Oxidation process occurred at the anodic reaction results in the reduction of steel due to producing electrons,

$$3\mathbf{F}e + 4\mathbf{H_2O} = \mathbf{F}e_\mathbf{3}\mathbf{O_4} + 8\mathbf{H}^+ + 8\mathbf{e}^- \tag{2.1}$$

$$2\mathbf{F}e + 3\mathbf{H}_2O = \mathbf{F}e_2O_3 + 6\mathbf{H}^+ + 6\mathbf{e}^- \tag{2.2}$$

$$\mathbf{F}e + 2\mathbf{H}_2O = \mathbf{H}FeO_2^- + 3\mathbf{H}^+ + 2\mathbf{e}^- \tag{2.3}$$

$$\mathbf{F}e = \mathbf{F}e^{+2} + 2\mathbf{e}^- \tag{2.4}$$

where anodic reactions depends on the presence of aggressive anions, the availability of a relevant electrochemical potential at the surface and the pH of electrolyte.

On the other hand, cathodic reaction results in forming hydroxyl ions reducing the dissolved oxygen,

$$\mathbf{2}H_2O + \mathbf{O}_2 + \mathbf{4}e^- = \mathbf{4}OH^- \tag{2.5}$$

$$\mathbf{6}H^+ + \mathbf{6}e^- = \mathbf{H}_2 \tag{2.6}$$

and it is a half-cell reaction depending on the existence of oxygen and on the pH of the reinforcement surface.

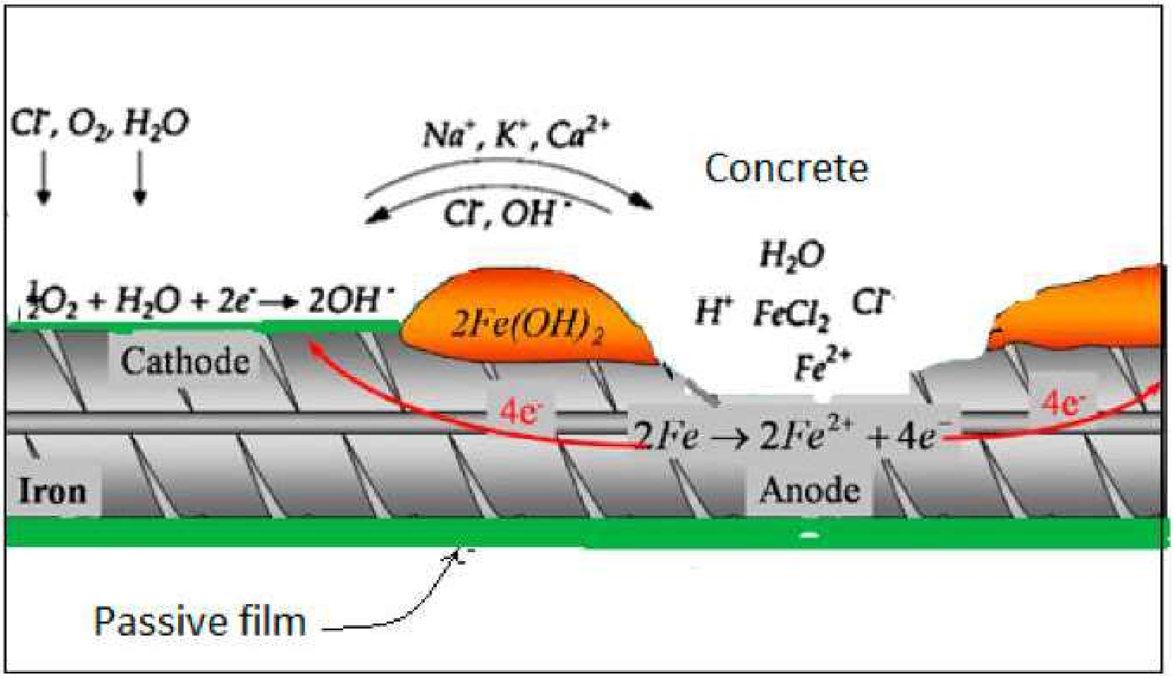

Figure 2.1. Schematic demonstration of the corrosion of steel bar in concrete (Naidu Gopu and Joseph, 2022).

The reaction happens with losing steel material and producing the rust which has generally 4 to 7 times larger volume. The increased volume produces stresses in concrete to an extent that it cracks, resulting in delamination and loss of concrete cover in RC members.

2.2. Factors Affecting the Corrosion Process of Steel Bars in Concrete

The factors affecting corrosion process of rebar in concrete can be divided into two categories. External factors cover the environmental parameters such as availability of oxygen and moisture at the rebar level, relative humidity and temperature, carbonation, and entry of acidic gaseous pollutants to rebar level, and chloride ions reaching to the rebar level either through the concrete ingredients or from the external environment.

On the other hand, internal factors include concrete and steel quality parameters such as cement composition, impurities in aggregates, impurities in mixing and curing water, admixtures, cement content, aggregate size and grading, construction practices, and chemical composition and structure of the reinforcing steel. The quality of concrete, mainly the permeability, nature and intensity of cracks, and the cover thickness, have also a great bearing upon the initiation and sustenance of reinforcement corrosion.

Corrosion process has three distinct stages. The first one is the De-passivation, and this process takes an initiation period. The next stage is the Propagation which starts from the time of de-passivation to the last one which is the Final State. Figure 2.2 schematically demonstrates the stages of the reinforcement corrosion.

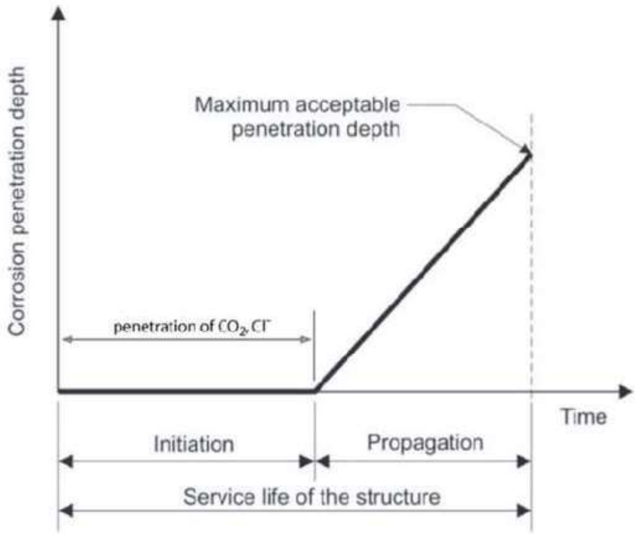

Figure 2.2. Stages of the reinforcement corrosion.

The primary structural effects of corrosion on the RC members can be summarized as:

- Decreased flexural strength,
- Ductility loss,
- Decreased high-cycle and low-cycle fatigue life and
- Reduced steel-concrete bond.

Effects of corrosion on the steel reinforcement and concrete are presented in Figures 2.3 to 2.7 (Concrete Preservation Technologies).

Figure 2.3. Effects of corrosion on reinforcement.

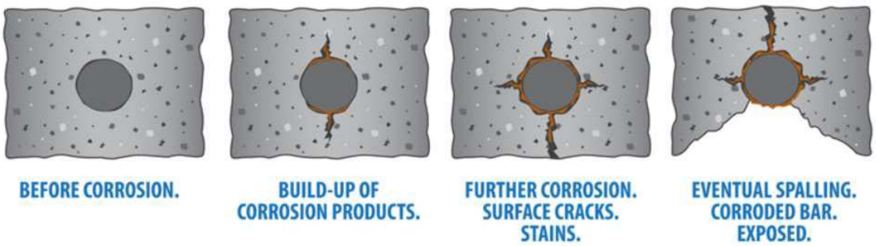

Figure 2.4. Effects of corrosion propagation on concrete.

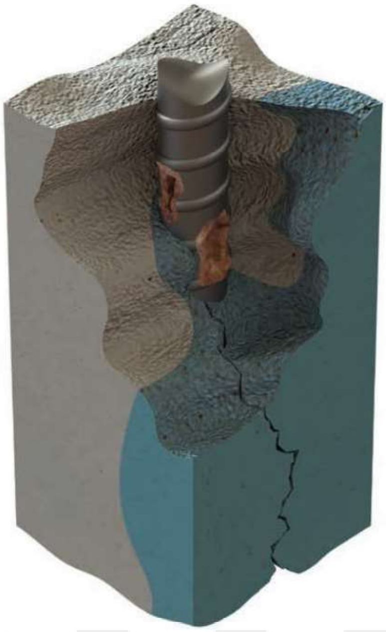

Figure 2.5. Demonstration of effects of corrosion on concrete.

Figure 2.6. Cracking of cover concrete due to corrosion.

Figure 2.7. Concrete spalling due to corrosion.

2.3. Diffusion Process

The time variant chloride content of the concrete significantly depends on the diffusion process that can be affected by several parameters such as concrete cover, the initial chloride content in the cement paste, chloride migration coefficient and critical chloride concentration that determines the corrosion initiation process presented in the Figure 2 (Bertolini et.al 2004). Therefore, the diffusion process can be modelled according to the Fick's Law of Diffusion and expressed as

$$\mathbf{C}(x=c,t) = \mathbf{C}_0 + (C_{s,\Delta x} - C_0)[1 - erf(\frac{c-\Delta x}{2\sqrt{D_{app,c(t)}}})] = \mathbf{c}_{crit} \tag{2.7}$$

$$\mathbf{D}_{app,c(t)} = \mathbf{D}_{RCM}(\frac{t_{28}}{t})^a \tag{2.8}$$

where c is concrete cover (mm), c_0 is the initial chloride content in the cement paste, Δx is the depth of the convection zone, $C_{s,\Delta x}$ is the chloride content (wt. % concrete), C_{crit} is the critical chloride content (wt. % concrete), D_{RCM} is the chloride migration coefficient (m^2/sec), $D_{app,c(t)}$ is the apparent coefficient of chloride diffusion, a is the aging coefficient, and t_{28} is the reference initial time (28 days).

The diffusion process is probabilistically expressed by assuming the primary parameters of the above equations as random variables with the distribution type, means and standard deviations presented in Table 2.1 (fib Bulletin N^o 34 2006). In addition, the initial chloride content in the cement paste and the depth of the convection zone are assumed as zero.

Table 2.1. Random variables.

Random Variable	**Distribution Type**	μ	σ
Concrete Cover (mm)	Normal	40	8
Chloride Migration Coefficient (m^2/s)	Normal	$15.8x10^{-12}$	0.20μ
Aging Coefficient (-)	Beta [0.0; 1.0]	0.3	0.12
Chloride Content (wt. %/cem.)	Normal	3	0.30μ
Critical Chloride Content (wt. %/cem.)	Beta [0.2; 2.0]	0.6	0.15

2.4. Corrosion Initiation Time

As presented in the Figure 2.2, deterioration due to corrosion appears in two stages which are corrosion initiation and corrosion propagation which can be described as follows (Stewart & Bastidas-Artega 2019):

Corrosion initiation:

- diffusion of aggressive agents through protective cover, and/or
- direct ingress of aggressive agents through cracks

Corrosion propagation:

- loss of cross-sectional area of reinforcing or prestressing steel,
- changes in ductility and mechanical properties of reinforcing or prestressing steel,
- reduction of bond, and
- crack initiation and propagation (spalling, delamination) caused by expansive rust products.

Corrosion propagation begins when the critical chloride content is reached at the surface of the reinforcements,

$$t_i = \frac{(c-\Delta x)^2}{4D_{RCM}}[erf^{-1}(\frac{c_{s,\Delta x}-c_{crit}}{c_{s,\Delta x}-c_0})]^{-2} \tag{2.9}$$

and corrosion initiation time can be calculated in accodance with the Fick's Law of Diffusion.

2.5. Effects of Corrosion on Reinforcing Bars

Corrosion leads to decrease in the effective cross-sectional area of reinforcing bars, which can be calculated taking the change in the mass account,

$$\mathbf{A_{cor}} = \mathbf{A_0}(1.0 - 0.01 * \mathbf{Q_{corr}}) \tag{2.10}$$

$$\mathbf{Q_{corr}} = \frac{\mathbf{M_0} - \mathbf{M_{corr}}}{M_0} * 100 \tag{2.11}$$

where A_0 is the initial net cross-sectional area of reinforcement, A_{cor} is the cross-sectional area of the corroded reinforcement, Q_{corr} is the corrosion level (%) of reinforcement, M_0 is the mass of non-corroded reinforcement, and M_{corr} the mass of the corroded reinforcement.

The second cause of the corrosion is the reduction of the yield strength of reinforcing steel along the building's service life. Therefore, the time-dependent yield strength of the corroded reinforcements should also be considered during the analysis (Du et.al 2005), where σ_y is the yield strength of non-corroded reinforcement, and $\sigma_y^{'}$ is the yield strength of the corroded reinforcement.

The last but not least, corrosion progress also causes the reduction of ductility capacity of reinforcing bars, and this phenomenon can be expressed by the ultimate strain (Zhang et.al 1995),

$$\sigma_y^{'} = \sigma_y(1.0 - 0.005 * Q_{corr}) \tag{2.12}$$

$$\epsilon_u = \epsilon_{uo}(1.0 - 0.0137 * Q_{corr}) \tag{2.13}$$

where ϵ_u is the ultimate strain of the corroded reinforcement, and ϵ_{uo} is the ultimate strain of non-corroded reinforcement.

2.6. Effects of Corrosion on Unconfined Concrete

Following the initiation of corrosion, the volume of the reinforcing bars starts to increase due to the accumulation of rust. The increased volume of the bars leads to the internal pressure on the cover concrete. As a result of this pressure cover concrete will crack. As a result, we can consider these causes in the analysis phase to calculate the loss of compressive strength (Molina et.al 1993; Coronelli & Gambarova 2004),

$$\sigma_c^r = \frac{\sigma_c^{'}}{1 + R\frac{\epsilon_a}{\epsilon_{co}}} \tag{2.14}$$

$$\epsilon_a = \frac{b_1}{b_0} - 1 \tag{2.15}$$

$$b_1 = b_0 + nw \tag{2.16}$$

$$w = \Sigma w_i = 2\pi x_b(V-1) \tag{2.17}$$

where $\sigma_c^{'}$ is the compressive strength of unconfined concrete with non-corroded bar, σ_c^r is the reduced compressive strength of unconfined concrete due to corrosion, ϵ_a is the average tensile strain in the cracked concrete, ϵ_{co} is the concrete strain at the compressive strain at $\sigma_c^{'}$, R is the coefficient related to the roughness and diameter of reinforcement, b_0 is the original width of the cross section, b_1 is the increased width due to corrosion cracks, w is the total crack width, w_i is the width of the i^{th} crack, x_b is the corrosion level, and V is the volumetric expansion ratio of the corrosion products.

2.7. Effects of Corrosion on Confined Concrete

Compressive strength and corresponding strain of the confined concrete can be expressed in terms of equivalent uniform confinement pressure provided by the tie reinforcement (Saatcioglu and Razvi 1992). Due to the decrease in the cross-sectional area and the yield strength, the confinement effect for the core concrete will be reduced. As a result of this process, the nonlinear stress-strain behavior of the confined concrete will change, its compressive strength and ductility will diminish. The reduced ductility of the confined concrete can be calculated utilizing the model proposed by Saatcioglu and Razvi 1992,

$$\sigma_c = f_{cc}[(\frac{2\epsilon_c}{\epsilon_{coc}}) - (\frac{\epsilon_c}{\epsilon_{coc}})^2]^{\frac{1}{1+2\lambda}} \leq f_{cc} \tag{2.18}$$

$$\sigma_c = f_{cc} + [(\frac{f_{cc} - 0.85f_{cc}}{\epsilon_{coc} - \epsilon_{c95}}](\epsilon_c - \epsilon_c) \geq 0.2f_{cc} \tag{2.19}$$

where σ_c is the compressive stress of confined concrete, f_{cc} is the compressive strength of concrete, ϵ_c is the compressive strain of confined concrete, and ϵ_{coc} is the ultimate compressive strain of concrete.

3. FUTURE CORROSION PROPAGATION

The main objective of this study is to propose a method to predict the future corrosion propagation of existing reinforced concrete buildings when the actual corrosion levels are determined by site inspections. For this purpose, Reverse Monte Carlo (RMC) method, which is a variation of the standard Metropolis–Hastings algorithm (Hastings 1970) and an effective tool to solve inverse problems, is used in the proposed procedure.

3.1. Monte Carlo Simulation

Monte Carlo simulation is an effective method to estimate reliable numerical results for any problems which have a probabilistic nature. It has been utilized in various real-life scenarios such as project management, financial forecasting, schedule estimations, signal processing, process design and telecommunication networks. Since it is a quite useful method for probabilistic risk analysis, it has been widely used in the seismic risk assessment studies too. Both the randomness of the seismic events and the material or modeling uncertainties are taken into account utilizing the Monte Carlo Simulation in the seismic risk assessment studies.

Park et.al. (1985) presented one of the earliest examples of the application of Monte Carlo simulation in the structural performance analysis of reinforced concrete buildings under earthquake excitations. They developed several single-degree-of-freedom and multi-degree-of-freedom systems representing both ductile and brittle RC structures. The developed systems were analyzed using Monte-Carlo Simulation method in order to consider the randomness of the earthquake vibrations.

Singhal and Kiremidjian (1996) proposed a probabilistic method for structural damage assessment of structures under seismic excitations. Since the nature of earthquake events and material properties of structures contains uncertainties, they used the Monte Carlo simulations to select the values of random input parameters required to carry out nonlinear time-history analysis as well as the capacity parameters such as compressive strength, damping ratio, geometrical information of the structural elements, area of the reinforcements and the yield strength of steel bars.

Shinozuka et.al (2002) conducted a reliability study in order to investigate the effects of retrofitting on the seismic vulnerability of concrete bridges. In order to identify the impacts of steel jacketing technique on the seismic performance of concrete bridges, they developed seismic fragility curves of the bridge before and after retrofit and they performed Monte Carlo simulation to determine the nonlinear dynamic performance of the bridges.

Hancilar et.al. (2014) conducted seismic vulnerability evaluation of public-school buildings located in Istanbul. This study is a good example of the application of Monte Carlo simulation for seismic performance assessment of buildings constructed according to generic or standard architectural and structural plans.

Zhong et.al (2016) performed a seismic risk analysis study for the cable stayed bridges located in the seismically active areas. They focused on the contribution of each component to the overall performance of the cable-stayed bridges and therefore used the Monte Carlo simulation to develop reliable system level fragility estimations. They utilized the Latin hypercube technique to create statistically different finite element models for bridges taking into account the material uncertainties. Monte Carlo simulation was performed to include the uncertainties related to earthquake direction, material properties, cross-sectional areas, span lengths, story heights and building mass.

Dukes et.al (2018) proposed a bridge-specific fragility estimation procedure which can provide useful information about the seismic performance of a bridge depending on the changes in the design parameters under various earthquake levels. They estimated the seismic performance of bridges of structural elements by considering the impact of design parameters via Monte Carlo Simulation and logistic regression analysis.

The deterioration of the structural elements can be considered as one of the main sources of the uncertainties related to seismic capacity. Therefore, in addition to randomness of the material and geometrical properties of structural elements, time-dependent changes have been also widely studied by other researchers. The causes of deterioration can be divided into to two main categories which are aging of the materials and the corrosion of steel reinforcements. They are dependent to internal and external factors which can be modelled via some mathematical equations containing various random variables.

Biondini and Frangopol (2008) carried out a probabilistic study in order to predict the lifetime of a reinforced concrete arch bridge. They consider the bending moment of the deck as the performance indicator, and they used the Monte Carlo simulation in order to determine the bending capacity of the structure for a 50-year period. The modeling parameters with uncertainties can be summarized as tension strengths of concrete and steel, reinforcement diameters, concrete and steel damage rates. In addition, they also modeled the dead and live loads as random variables to have a more reliable probabilistic analysis. Finally, in order to determine the lifetime performance of the bridge, corrosion was considered as the primary cause of the deterioration and the diffusion coefficient was used in the Monte Carlo simulations.

Ghosh and Padgett (2010) developed a time-dependent fragility curves of concrete bridges exposed to corrosion. They followed a fully probabilistic methodology utilizing the Monte Carlo Simulation in order to develop the seismic fragility curves of bridges. The random variables considered for the structural analyses included the material properties of the structural elements, ground motions used as the input for dynamic analyses and parameters related to corrosion diffusion process.

Kumar and Gardoni (2014) examined the structural deterioration of reinforced concrete highway bridges and the impacts of degradation on the seismic vulnerability of bridges located in the seismically active areas. They used the Monte Carlo simulation to integrate the seismic performance assessment with the structural degradation due to corrosion.

Although existing literature on the application of Monte Carlo simulations for seismic performance estimations presents valuable information about the corrosion process, its uncertainties and life-cycle performance analysis and cost forecasts related to infrastructure management, there is still a need to integrate the corrosion levels of existing structures, identified via monitoring or site inspections. Therefore, this study aims to present the Reverse Monte Carlo method which can be used to predict the future corrosion propagation of reinforced concrete structures in accordance with the existing corrosion levels identified by site inspections.

3.2. Reverse Monte Carlo

Reverse Monte Carlo can be applied to various sorts of data and aims to obtain a model or a set of models which complies with the available measurements or experimental data and any information provided as constraints (McGreevy 2001).

Müller et.al. (2010) employed the Reverse Monte Carlo method to verify the structural information created by molecular dynamics simulation of glass. Timoshenko et.al. (2012) presented application of Reverse Monte Carlo method developed to investigate the local disorders in crystalline materials by adjusting the wavelet transform of the extended X-ray absorption structure signal. Da et.al (2013) utilized the Reverse Monte Carlo method to obtain bulk energy loss function from reflection electron energy-loss spectroscopy data. Temleitner (2014) performed Reverse Monte Carlo method in order to discover the structural information about the liquid carbon tetrabromide in compliance with X-ray and neutron diffraction data. Di Cicco and Iesari (2022) proposed a Reverse Monte Carlo method to develop 3-dimensional models of exemplary molecular and condensed systems.

When using the RMC method, the random parameters of a numerical model (such as the diffusion process model) is adjusted until the results / predictions (i.e., the corrosion levels of existing buildings) have the maximum consistency with experimental data (the existing corrosion levels identified via site inspections).

The novelty of the proposed method is to use existing corrosion levels of the reinforcements to make more reliable predictions for the future corrosion propagation. In other words, site measurements or monitoring results can be considered as the reference data according to which numerical models used to predict corrosion propagation are validated. As a result, the proposed method will provide future corrosion propagations which comply with the existing corrosion levels.

The process of the RMC can be described as follows:

- the process starts with the standard Monte-Carlo Simulation to predict the corrosion level of an existing building
- the predicted corrosion levels are compared with the experimental measurements (existing corrosion level) using the following equation in order to eliminate the predictions which are inconsistent with measurements
- in accordance with the predictions complied with existing corrosion levels, the values and applicable combinations of random variables presented in the Table 1 are determined
- using the identified values of corrosion initiation time, concrete cover, chloride mitigation coefficient, aging coefficient, chloride content and existing corrosion levels, the future corrosion propagations are estimated,

$$X_0^2 = \Sigma(C^p - C^t)^2/\sigma^2 \tag{3.1}$$

where X_0 is the error, C^p is the corrosion levels predicted via diffusion process model, C^t is the existing corrosion levels determined via site inspections, and σ is the test error.

The procedure of using the Reverse Monte Carlo method to estimate the future corrosion propagation of existing structures is presented in the Figure 3.1.

The difference between the corrosion estimation via Monte Carlo Simulation and predicting the future corrosion propagation using Reverse Monte Carlo is presented in figures 3.2 and 3.3. As presented in the Figure 3.3, when the existing corrosion level is identified via site inspections, it is possible to eliminate the non conforming predictions presented in the Figure 3.3. Afterwards, the future corrosion propagation can be estimated using the predicted corrosion levels complying with the experimental results.

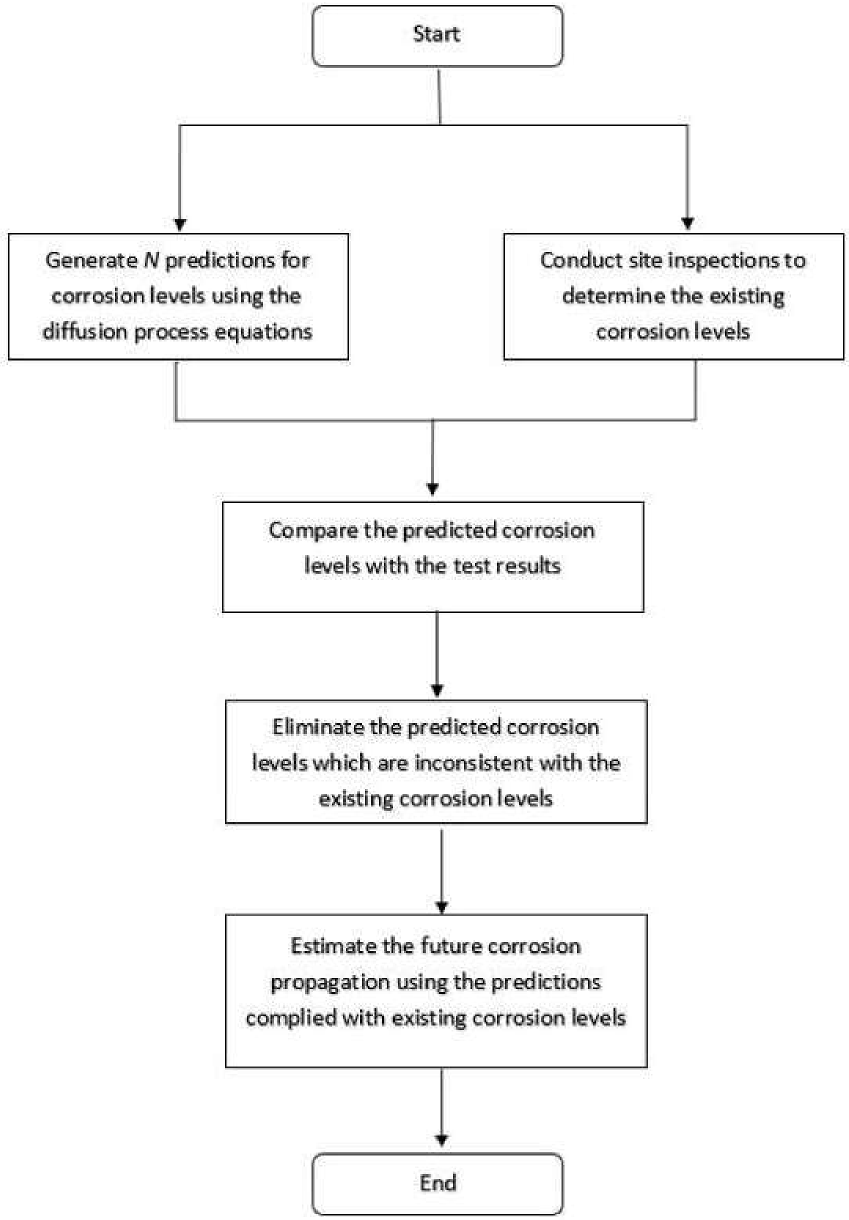

Figure 3.1. RMC method to estimate future corrosion propagation.

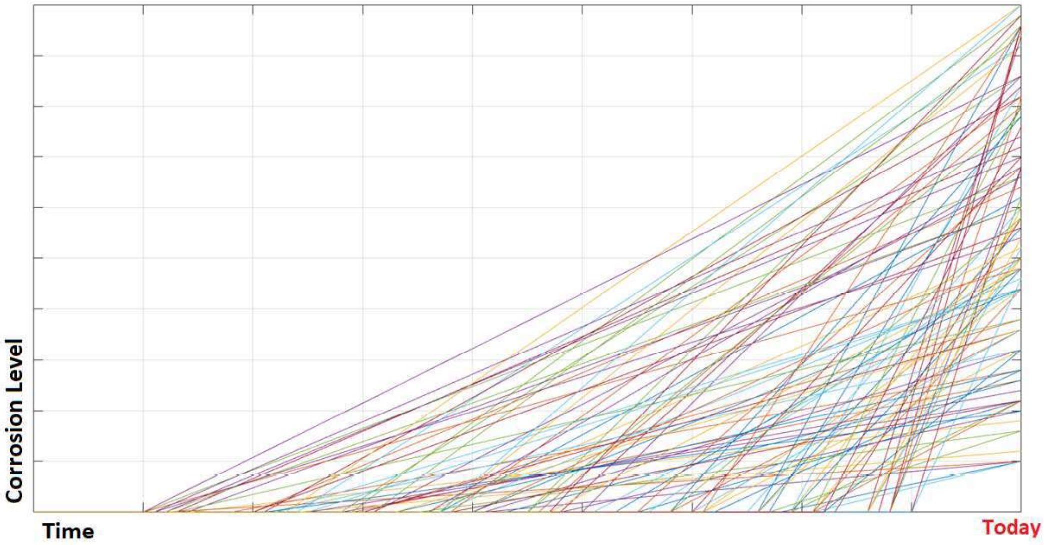

Figure 3.2. Monte-Carlo simulation to predict today's corrosion level.

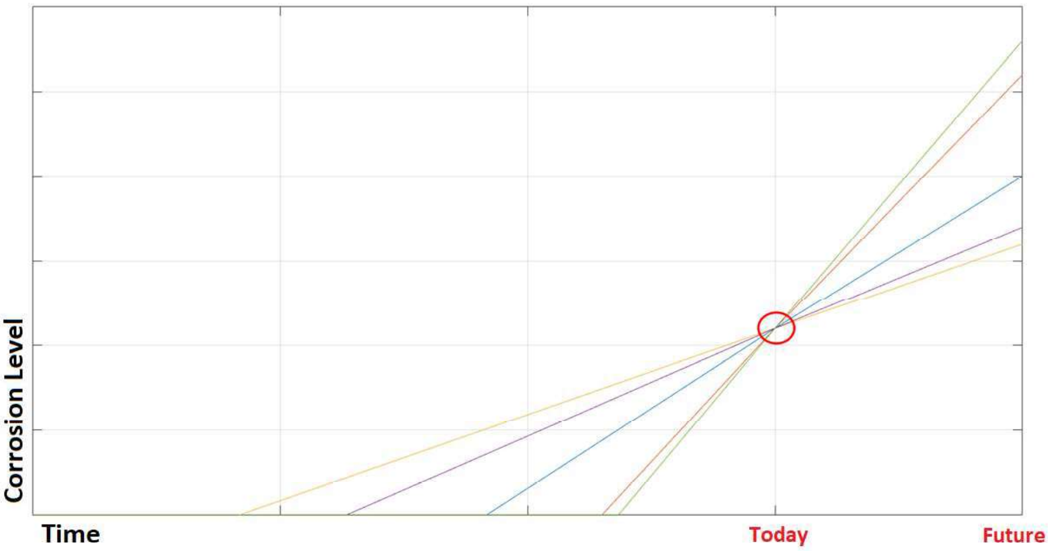

Figure 3.3. Future corrosion propagation using RMC.

4. CASE-STUDY: TIME-DEPENDENT SEISMIC PERFORMANCE OF RC BUILDINGS

4.1. Building

A corroded reinforced concrete building located in New Zealand and constructed in 1928 is considered here in order to present the effectiveness of the proposed method (Nataraj et.al 2020; Nataraj et.al 2021). The aim is to predict the future corrosion propagation taking into account the existing corrosion levels determined by the site inspections. The case study building has a plan area of 24.675 m × 12.825 m, with a 150 mm slab thickness. The four-story west elevation had a floor height of 4.5 m, the width of Bay 1 was 3.725 m, and the widths of Bays 2 and 3 were 4.175 m each. The plan and elevation views of the building are presented in Figure 4.1. In addition, cross-section details of the beams and columns are presented in Figure 4.2 and Figure 4.3, respectively (Nataraj et.al 2021).

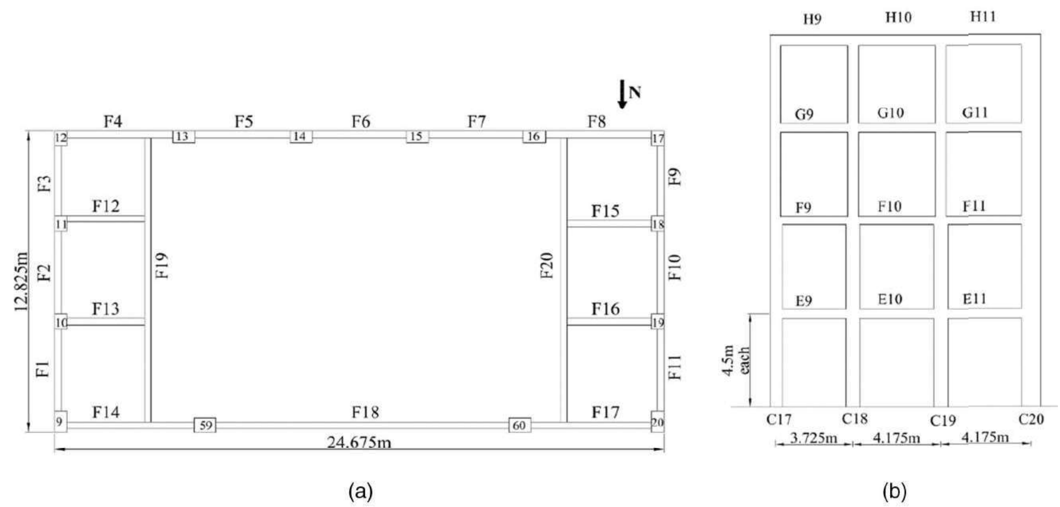

Figure 4.1. Layout of the case study building: (a) plan; (b) elevation (Nataraj et.al 2021).

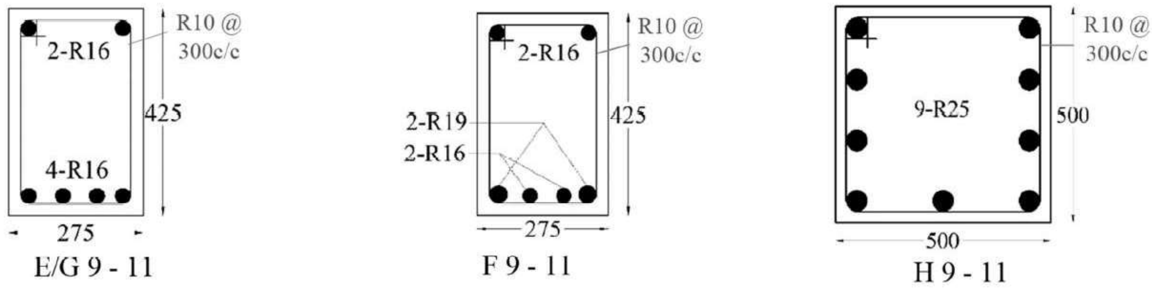

Figure 4.2. Cross-sections of the beams (Nataraj et.al 2021).

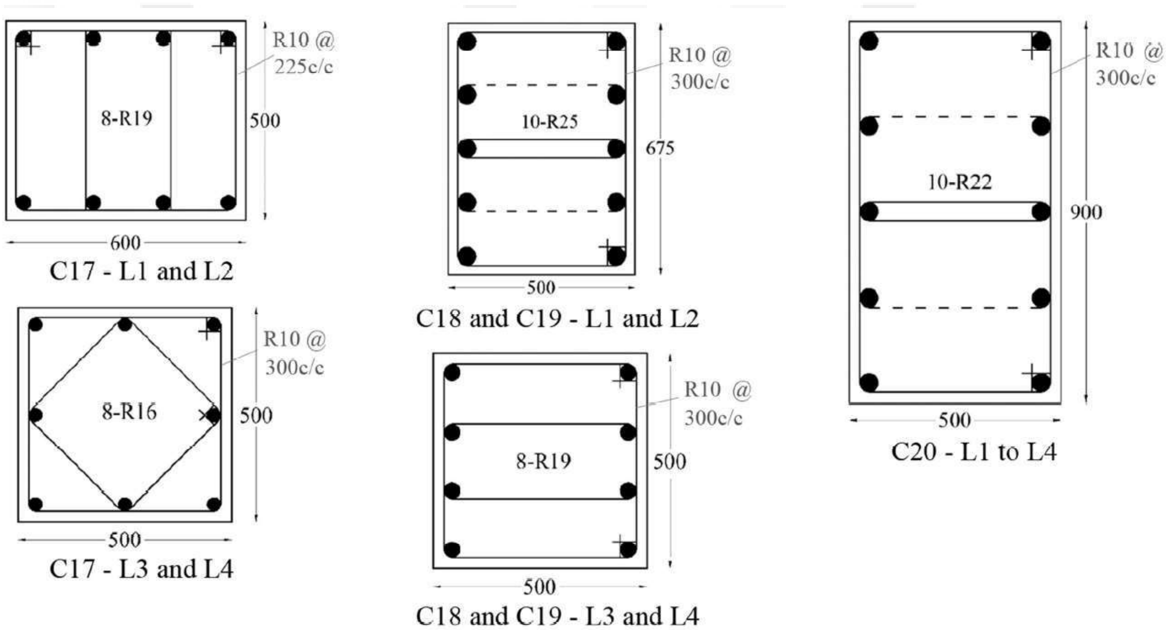

Figure 4.3. Cross-sections of the columns (Nataraj et.al 2021).

The reduction in the cross-sectional area of the reinforcing bars was measured using manual calipers on site following the removal of surface rust. The identified cross-sectional loss was used at the locations in which concrete spalling occurred, since the direct measurements were possible. In locations where only longitudinal cracking was observed, in other words it was not possible to take direct measurements, as a conservative approach, the foregoing measured average cross-sectional loss of reinforcements was used for assessment. The average loss of cross section of the longitudinal bars was determined as 12% with COVs of 0.30 (Nataraj et.al 2021).

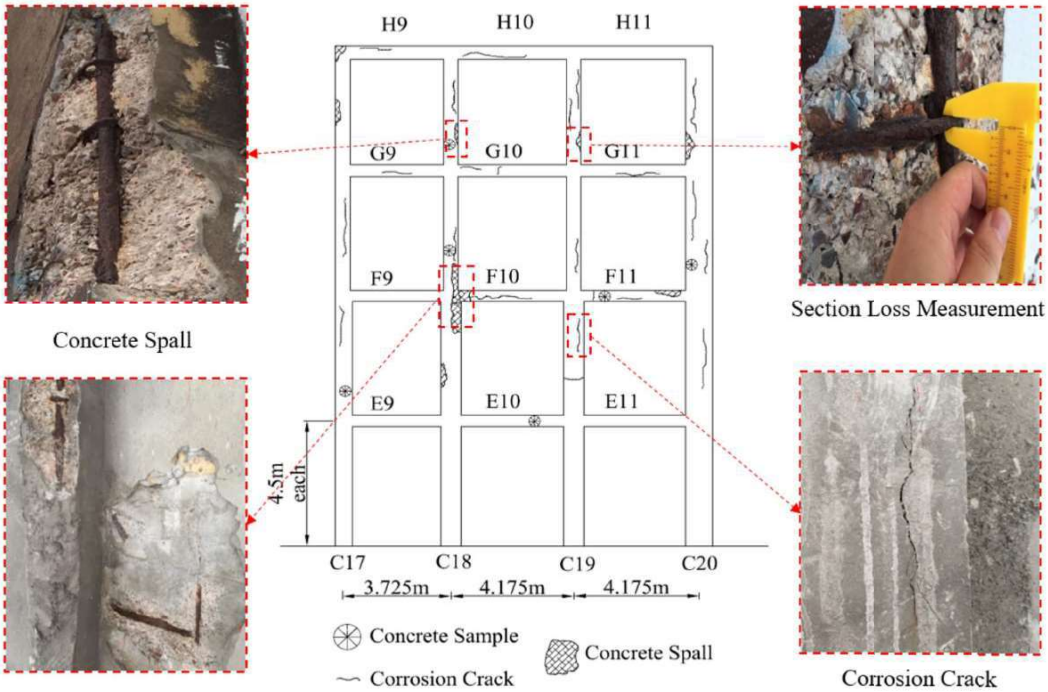

Figure 4.4. Condition assessment of the case study building (Nataraj et.al 2021).

4.2. Corrosion Propagation

In order to estimate the future corrosion propagation of the building, RMC method was utilized. At the first step of this method, acceptable difference between the predicted and existing corrosion levels was assigned as 1%. The diffusion process for the chloride ions were modeled using the following equations 2.7 and 2.8 representing the Fick's Law of Diffusion.

The probabilistic distributions of the parameters such as depth of the cover concrete, chloride migration coefficient, aging coefficient, chloride content and critical chloride content, taken into account in this model and presented in Table 2.1, were considered in the analyses. Moreover, cement paste's initial chloride content and the convection zone depth were taken as zero.

Using these parameters and the diffusion process model, 100000 corrosion predictions were obtained. The predicted corrosion levels were compared with the corrosion levels investigated via site inspections in accordance with the equation 3.1.

The corrosion level estimations which are consistent with the site measurements were classified as suitable, which means that they can be used as the reference points to predict the future corrosion propagation of the steel reinforcements. On the other hand, the predictions which did not comply with the corrosion levels determined via site inspections were not included in further analyzes. This process can be mentioned as the first phase or first step of the Reverse Monte Carlo for corrosion prediction and the details of this phase are summarized in the Table 4.1.

Table 4.1. Summary of the RMC process.

# of Prediction	100000
Average Corrosion Level	12%
COV	0.3
Accepted Error Level	1%
# of Complied Prediction	66

In addition to summary, Figure 4.5 shows the graphical comparison of distribution obtained by field measurement and prediction obtained via Reverse Monte Carlo simulation. Furthermore, in order to make quantitative comparison between these distributions, their skewness and kurtosis values were calculated, and these values are presented in Table 4.2.

As it can be observed from Figure 4.5 and Table 4.2, the distribution of corrosion levels predicted by utilizing Reverse Monte Carlo method is quite similar to the one determined by field measurements. Therefore, it can be claimed that using the combinations identified via the procedure presented in Figure 3.1, the future corrosion propagation of the building can be estimated reliably.

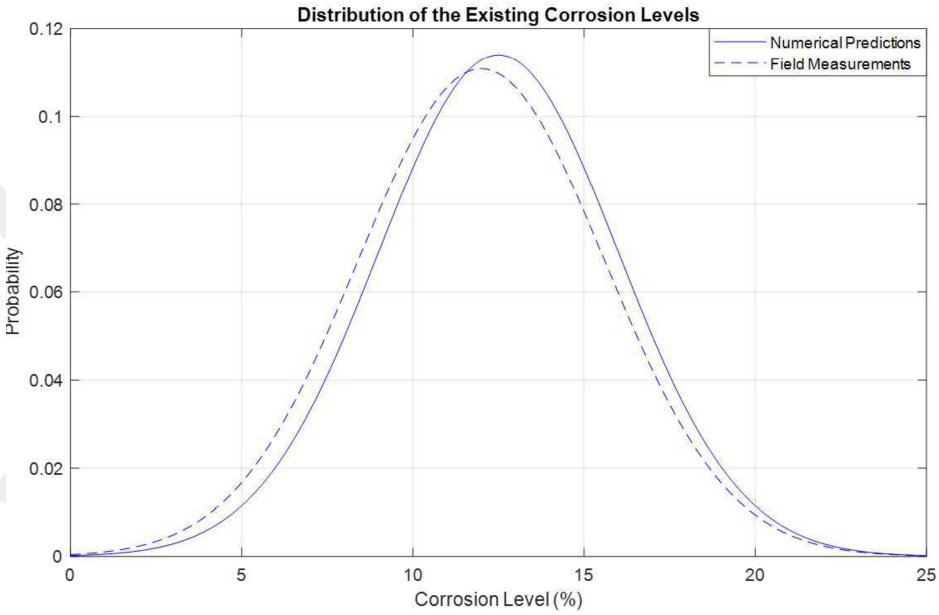

Figure 4.5. Comparison of the distribution of corrosion levels.

Table 4.2. Skewness and kurtosis of distributions.

Data Type	**Skewness**	**Kurtosis**
Field Measurement	0.59	1.81
Numerical Predictions	0.63	1.85

The second phase of the analysis is to estimate the future corrosion propagation as presented in the Figure 3.1. For this purpose, two outputs of the previous step were utilized as the inputs. The first one is definitely the predicted values for the existing corrosion level. The second input was the combinations of the random variables of the equations 2.7 and 2.8, which gave the estimations for corrosion levels that were consistent with the site inspection results. As a summary, the suitable corrosion predictions can be specified as the starting point of the last phase whereas the values of the random parameters enabling to reach these predictions can represent the path that must be followed.

In order to identify the change in the time-dependent seismic performance of this building, 10-year time-intervals were selected. Therefore, future corrosion propagation were estimated for the next 10, 20, 30, 40 and 50 years of the building. The distributions of the estimated future corrosion levels of the building for 10 to 50 years later are presented in Figures 4.6 to 4.10.

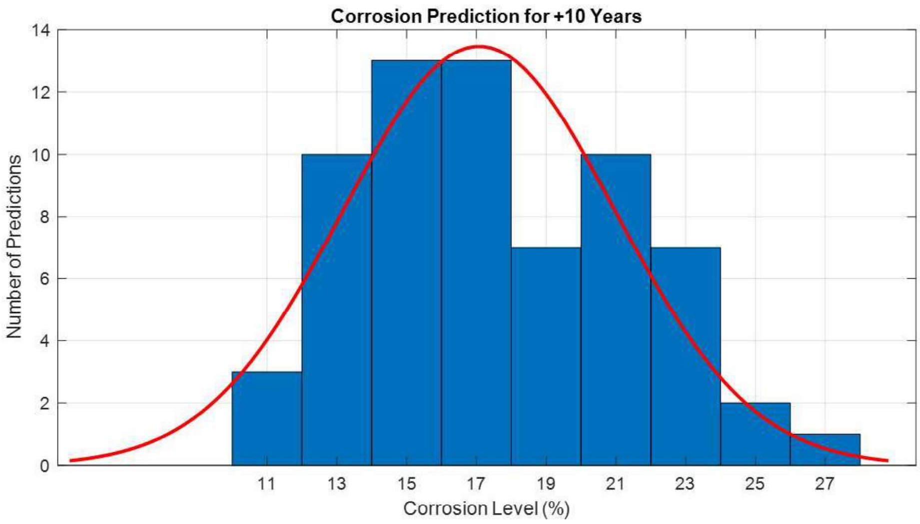

Figure 4.6. Corrosion predictions for 10 years later.

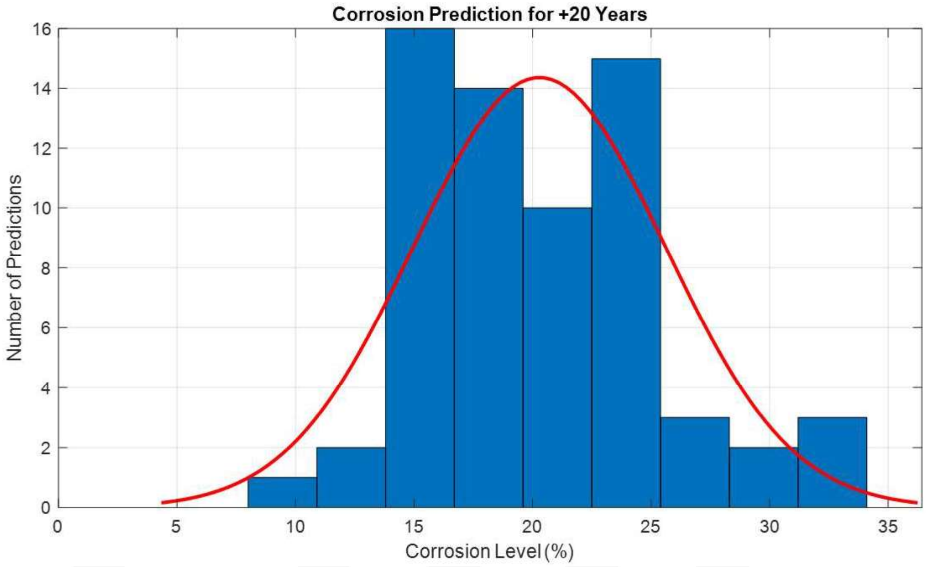

Figure 4.7. Corrosion predictions for 20 years later.

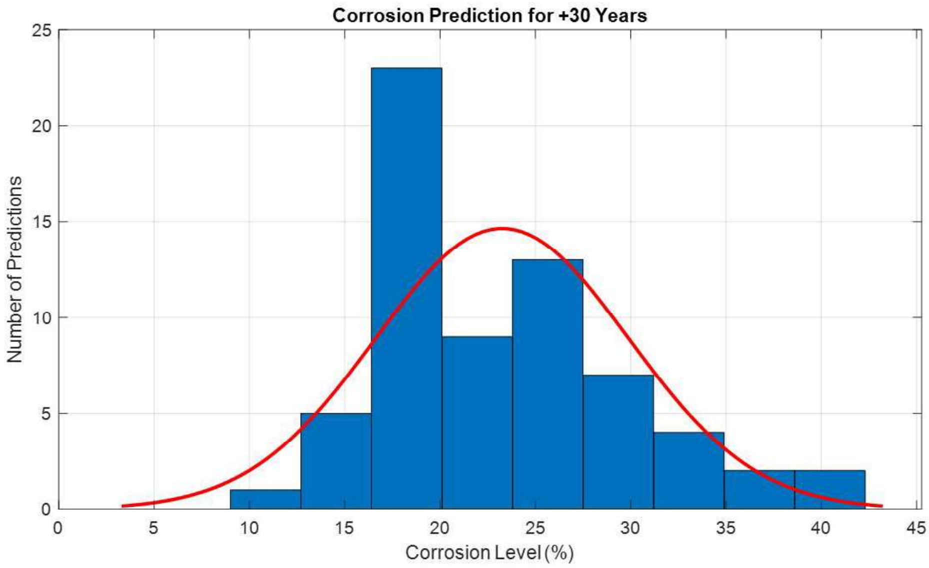

Figure 4.8. Corrosion predictions for 30 years later.

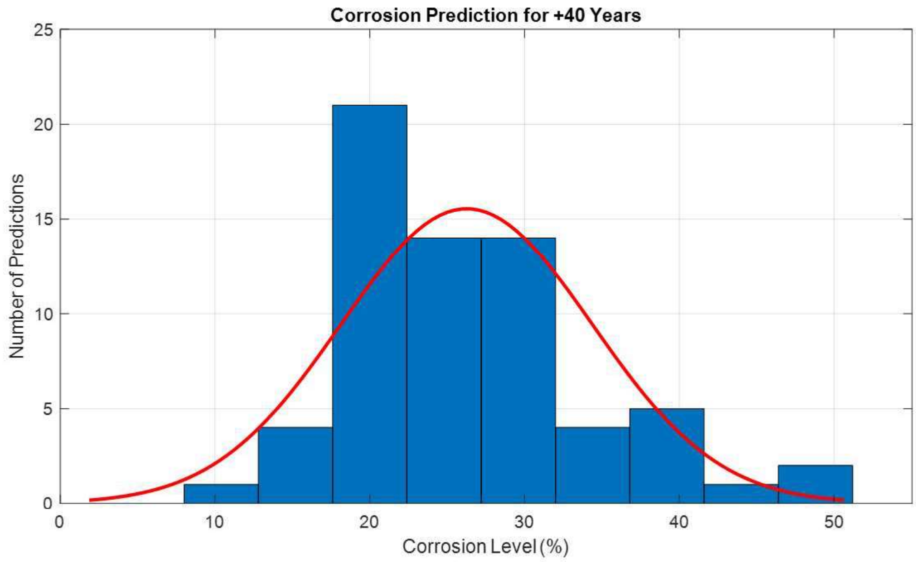

Figure 4.9. Corrosion predictions for 40 years later.

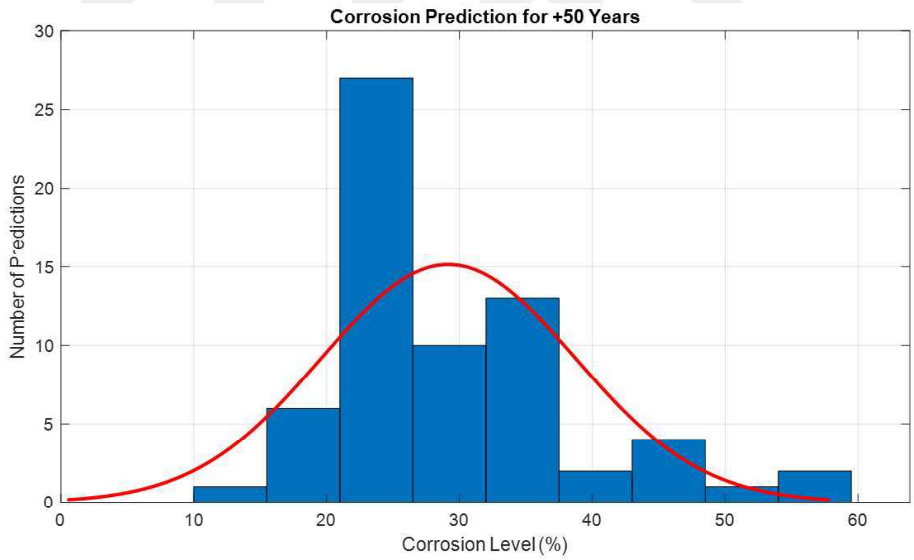

Figure 4.10. Corrosion predictions for 50 years later.

4.3. Structural Modeling

4.3.1. OpenSees

OpenSees (Mazzoni et.al., 2006) was used in this study to conduct a series of structural analyses that can be used to estimate the time-dependent seismic performance of the building subjected to corrosion.

OpenSees can be defined as "a software for creating applications for the nonlinear analysis of structural and soil systems using either a standard FEM or an FE reliability analysis". It follows the object-oriented programming structure which means that the software can be recognized as collection of the various objects. These objects can communicate effectively during the structural analysis by sending and receiving messaged from each other and processing data provided by other objects as the inputs (McKenna 2011).

OpenSees has an extendable and transformable programming structure, therefore its flexibility allows the users to achieve high level of efficiency during the computational efforts for the complex systems.

Main section of the OpenSees can be summarized as follows:

- Model Builder: the section which is used to create the Finite Element Model of the structure or system under investigation
- Analysis: apply predefined changes / loads to model in order to move the system from state at time (t) to time (t + dt)
- Recorder: another critical section of the OpenSees because parameters such as stress, strain, displacement, rotation, or loads defined by the user prior to analysis were monitored and recorded by the elements of this section during the analysis
- Domain: this section holds the states of the model at different times

4.3.2. Material Model of Reinforcing Bars

The reinforcing bars were modeled using the uniaxial material model ReinforcingSteel which can incorporate buckling (Brown & Kunnath 2006). This model has two main parts, the first of which is related to mechanical properties of the steel. The second part of the model contains several parameters that can be used to modify the buckling, low-cycle fatigue, strength reduction and isotropic hardening of the reinforcing bars.

The actions taken to represent the changes in the mechanical properties and cross-sectional areas of the reinforcements due to adverse impacts of corrosion are presented below:

Yield stress in tension: the initial value for the uncorroded reinforcements was taken from the Table 4.4. Afterwards, estimated future corrosion levels were used in the equation 2.12 in order to predict the yield strength of the corroded reinforcing bars.

Ultimate stress in tension: the initial value for the uncorroded steel bars was obtained from the Table 4.4. Similar to the yield stress, the estimated corrosion levels were used in order to calculate the ultimate strength of the corroded reinforcements.

Yield strain in tension: this value is calculated by the OpenSees in accordance with the inserted yield stress and elastic modulus values. Since these properties were calculated and updated in the software for different corrosion levels, the changes in yield strain due to corrosion were taken into account too.

Ultimate strain in tension: the starting point for the ultimate strain at the uncorroded stage was determined according to Table 4.4. Afterwards, equation 2.13 was used to calculate the ultimate strain capacity of reinforcements at different corrosion levels.

Elastic modulus: similar to stress and strain values, the initial elastic modulus was taken from the Table 4.4 and the effects of corrosion on this property was estimated.

Slenderness ratio: the spacing between tie reinforcements were used to calculate the slenderness ratio of the uncorroded structure. The change in the cross-sectional area of these bars due to corrosion were calculated and the slenderness ratios for different corrosion levels were estimated accordingly. However, it is meaningful to state that since the initial slenderness ratio of the columns were big, the negative impacts of the corrosion of ties cannot be observed effectively.

4.3.3. Material Model of Unconfined Concrete

Unconfined concrete were modeled using the Concrete04 material model which uses Popovic's curve (Popovic 1973) in compression and a linear-exponential decay curve in tension.

It is a well-known fact that once the corrosion initiates, the volume of the steel reinforcements starts to expand due to rust accumulated on the steel bars. Therefore, there will be an internal pressure on the cover concrete due to increased volume of the reinforcing bars. This internal pressure will cause cracking of unconfined concrete and as a result, the compressive strength of the cover concrete will decrease.

The Concrete04 material model requires the inputs related to following properties in order to simulate the concrete behavior:

Compressive strength: the initial value of compressive strength without corrosion effects were taken from Table 4.3. Afterwards, equation 2.14 was used to calculate the compressive strength reduced due to corrosion.

Tensile strength: Table 4.3 presents the tensile strength value of the concrete before the corrosion initiated on the reinforcing bars. The equation provided by American Concrete Institute (ACI) Code (2008) was used in this study in order to calculate the tensile strength of unconfined concrete,

$$f_{ct} = 0.63\sqrt{f_c} \tag{4.1}$$

where f_{ct} is the tensile strength of concrete and f_c is the compressive strength of concrete.

Elastic modulus: for the uncorroded structure, the elastic modulus value presented in Table 4.4 was used in the material model. Since the elastic modulus of concrete is associated with its compressive strength, commonly used equation provided by American Concrete Institute (ACI) Code (2008) was utilized in this study in order to calculate it after corrosion initiation,

$$E_c = 4700\sqrt{f_c} \tag{4.2}$$

where E_c is the modulus of elasticity of concrete, and f_c is the compressive strength of concrete.

4.3.4. Material Model of Confined Concrete

Similar to the unconfined concrete, Concrete04 material model was selected to model the confined concrete in OpenSees. However, unlike the unconfined concrete, the calculation phase of the mechanical properties of confined concrete can be divided into two phases.

During the first phase, the same process with unconfined concrete was followed.

Compressive strength: the initial value of compressive strength without corrosion effects were taken from Table 4.3. Afterwards, equation 2.14 was used to calculate the compressive strength reduced due to corrosion.

Tensile strength: Table 4.3 presents the tensile strength value of the concrete before the corrosion initiated on the reinforcing bars. In order to calculate the tensile strength of confined concrete, the equation 4.1 provided by American Concrete Institute (ACI) Code (2008) was used.

Elastic modulus: for the corroded structure, the elastic modulus value presented in Table 4.4 was used in the material model. Since the elastic modulus of concrete is associated with its compressive strength, equation 4.2 provided by American Concrete Institute (ACI) Code (2008) was used in order to calculate it after corrosion initiation.

On the other hand, since the presence of horizontal reinforcements can have significant impacts on the compressive strength and ductility capacity of confined concrete, the first phase mentioned above is not sufficient to model the mechanical properties of confined concrete.

Saaticioglu and Razvi model (Saatcioglu and Razvi 1992) was used in this study to simulate the stress - strain behavior of confined concrete.

In addition to confinement effects on the mechanical properties of confined concrete, the negative effects of corrosion of tie reinforcements must be taken into account too. Due to the decrease in the cross-sectional area and the yield strength of horizontal reinforcements, the confinement effect for the core concrete will be reduced. Therefore, the nonlinear stress-strain behavior of the confined concrete will change, its compressive strength and ductility will diminish. The reduced ductility of the confined concrete can be calculated using the equations 2.18 and 2.19 (Saatcioglu and Razvi 1992).

It is important to note that the slenderness ratio of the columns of the case-study building considered in this study is high even for intact stage of the building, the adverse impacts of changes in the confinement effect cannot be observed properly, especially for the ductility capacity. In other words, confinement effects of the uncorroded structure is not sufficient enough to represent the huge decreases in the ductility capacity due to corroded tie reinforcements.

Table 4.5 presents the maximum decreases in the ductility capacities of confined concrete for different column types.

Table 4.3. Material properties - concrete.

Property	**Value**
Compressive Strength (MPa)	25.5
Tensile Strength (MPa)	2.25
Elastic Modulus (MPa)	23229
Ultimate Compressive Strain (Unconfined Concrete)	0.004

Table 4.4. Material properties - steel.

Property	**Value**
Yield Strength (MPa)	300
Elastic Modulus (MPa)	200000
Yield Strain	0.15%
Ultimate Strength (MPa)	375
Ultimate Strain	20%

Table 4.5. Change in ductility levels of core concrete.

Column Type	**Value**
C17 - (1st and 2nd floor)	35.3%
C17 - (3rdt and 4th floor)	26.6%
C19 - (1st and 2nd floor)	26.6
C19 - (3rdt and 4th floor)	21.4%
C20	20%

4.3.5. Modeling of Columns and Beams

Material non-linearity is one of the most important topics in finite element modeling in order to assess the seismic performance of structures effectively. The modeling options for material non-linearity can be divided into two categories which are concentrated and distributed plasticity.

Figure 4.11 presents the idealized beam-column models considering both concentrated and distributed plasticity.

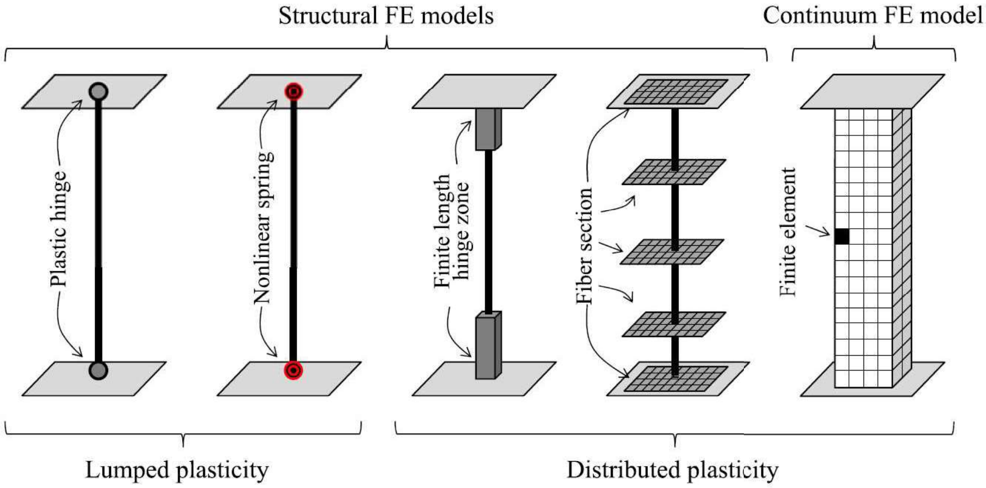

Figure 4.11. Idealized beam-column models considering both concentrated and distributed plasticity (Astroza et.al. 2015).

Concentrated plasticity is an approach that includes the placement of zero-length hinges at the ends of structural elements to represent or capture the plastic deformations concentrated mainly on these portions of columns and beams. Specific load-deformation relation, either force-displacement or moment-rotation, is assigned to these plastic hinge elements to monitor and record the load and deformation histories throughout the nonlinear analyses.

The most important advantage of this modeling option is that it is a simple and lightweight technique and also requires relatively less computational efforts to run a nonlinear analyses, especially for large and complex systems. However, it cannot record the interaction between bending moment and axial force or capture the plasticity that may occur at any locations other than the end of structural elements. Moreover, the main purpose of this study is to present the effects of corrosion and it is not possible to effectively capture the impacts on corrosion on the nonlinear behavior of structural elements.

On the other hand, the distributed plasticity model can simulate the variations of the stress and strain through the section and along the structural element in more detail. Critical local behaviors, such as strength degradation due to local reinforcement buckling, or the nonlinear interaction of flexure and shear, can be captured with sophisticated and numerically intensive models. Therefore, in this study, distributed plasticity approach was selected to model the non-linearity of structural elements.

For this purpose, columns and beams were modeled via Displacement-Based Beam-Column element available in the OpenSees, since it permits spread of plasticity along the element and therefore it allows yielding to occur at any location along the element. Quadrilateral line sections were defined in accordance with the Figures 4.2 and 4.3 and using the pre-defined material models before developing the displacement-based beam-column elements.

Figure 4.12 presents the three-dimensional visualization of the OpenSees model.

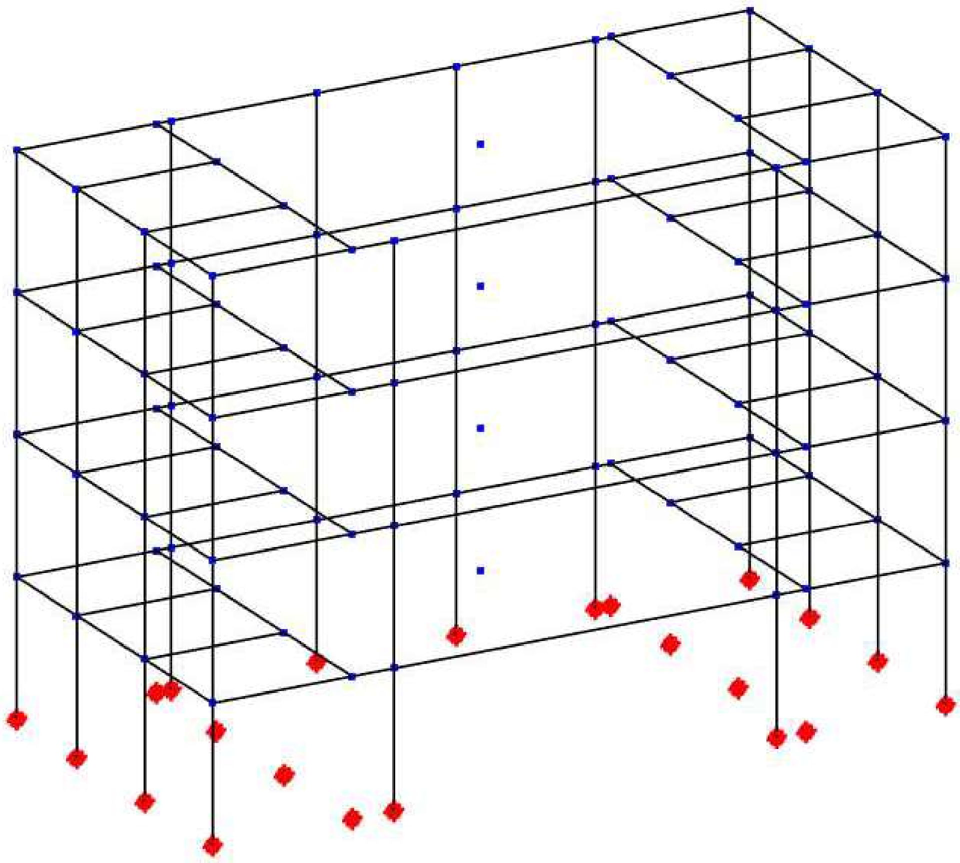

Figure 4.12. Three-dimensional visualization of the OpenSees model.

4.4. Nonlinear Static Analysis

In order to determine the displacement demands used in the nonlinear static analyses, Turkish Seismic Design Code 2018 was used as the guidance. The earthquake level DD-1 that has a return period of 2475 years was considered in this study and a random location in Istanbul was selected to determine the parameters such as horizontal elastic design spectral acceleration, design spectral acceleration coefficient for the short period region, and design spectral acceleration coefficient for period of 1.0 seconds required to develop the design spectrum (TSDC 2018).

The impacts of corrosion of reinforcing bars on the modal parameters of structural elements have been examined by other researchers and the decrease in natural frequencies, in other words increase in natural periods, has been reported (Abdul Razak & Choi 2001 and Duvnjak et.al. 2021). Therefore, in order to represent the effects of corrosion on the seismic demand, changes in natural periods of the building were predicted via finite element model. Tables 4.6 and 4.7 present the modal analyses results and the related displacement demands utilized in the nonlinear static analyses.

The design spectrum used as the reference for nonlinear static analyses and a capacity spectrum obtained via analyses are presented in Figure 4.13.

Table 4.6. Natural periods of the building in EW direction.

Corrosion Level	T_x **(sec)**	Sd_x **(m) - EW**
No Corrosion	1.12	0.110
Existing Condition	1.33	0.131
10%-15%	1.34	0.132
15%-20%	1.34	0.133
20%-25%	1.35	0.134
25%-30%	1.36	0.135
30%-35%	1.37	0.136
35%-40%	1.38	0.137
40%-45%	1.39	0.138
45%-50%	1.41	0.139
50%-55%	1.42	0.14
55%-60%	1.43	0.141

Table 4.7. Natural periods of the building in NS direction.

Corrosion Level	T_y **(sec)**	Sd_y **(m) - NS**
No Corrosion	2.05	0.199
Existing Condition	2.62	0.258
10%-15%	2.63	0.259
15%-20%	2.66	0.262
20%-25%	2.69	0.265
25%-30%	2.72	0.268
30%-35%	2.76	0.272
35%-40%	2.79	0.275
40%-45%	2.83	0.279
45%-50%	2.87	0.283
50%-55%	2.9	0.286
55%-60%	2.93	0.289

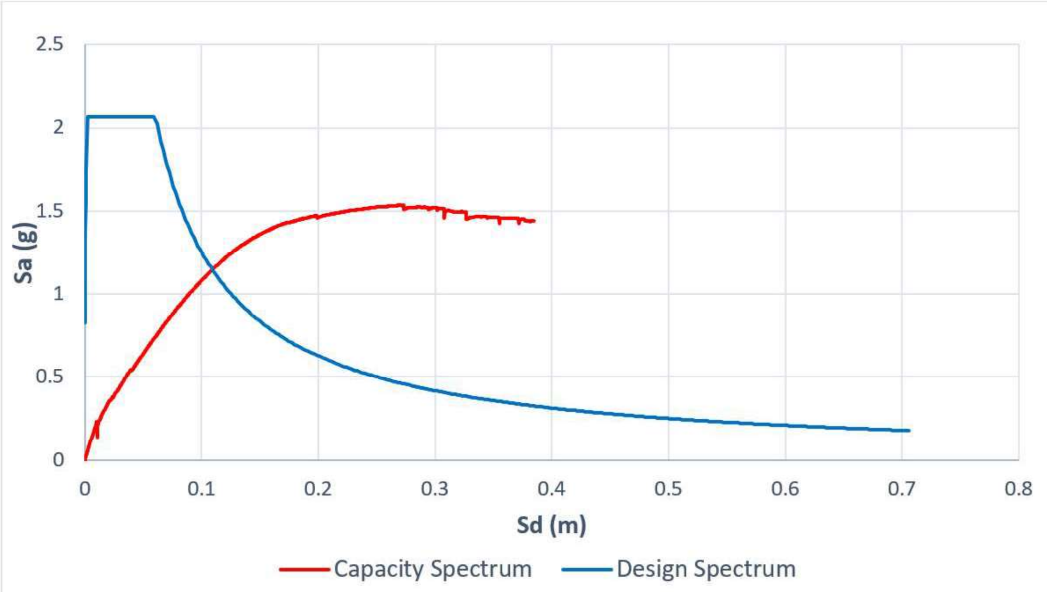

Figure 4.13. Design spectrum vs capacity spectrum.

Drift ratio was considered as the performance indicator to estimate the seismic performance of the building. Figures 4.14 and 4.15 show the drift ratios in East-West and North-South directions, respectively. It can be noticed that there is a moderate increase in the drift ratios in East-West direction whereas the drifts in the North-South direction changes more significantly. Therefore, it can be claimed that the seismic performance of the building mostly depends on the structural responses in the North-South direction.

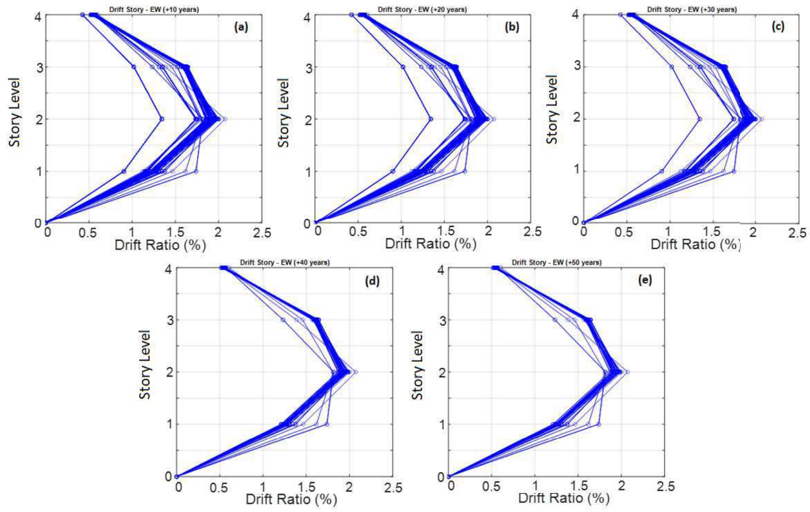

Figure 4.14. Drift ratios in the east-west direction: (a) 10 years later, (b) 20 years later, (c) 30 years later, (d) 40 years later, (e) 50 years later.

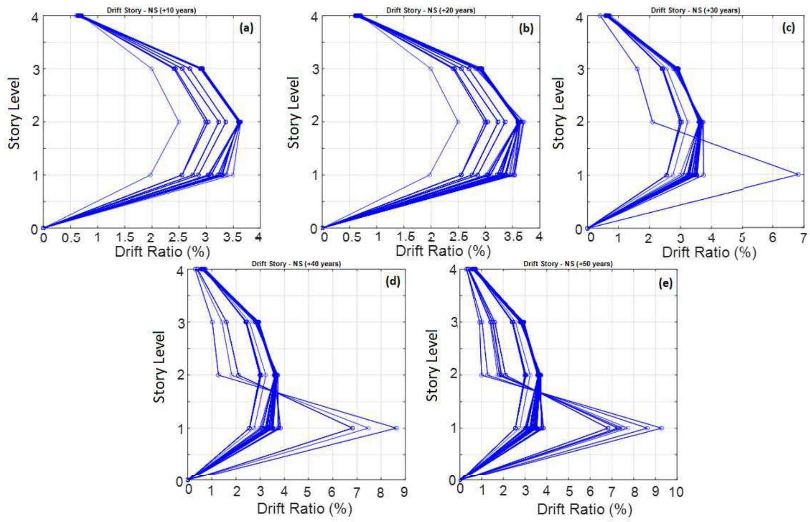

Figure 4.15. Drift ratios in the north-south direction: (a) 10 years later, (b) 20 years later, (c) 30 years later, (d) 40 years later, (e) 50 years later.

As presented in the Figure 4.15, starting from +30 years, a significant increase in the drift ratio of the first story was recorded in the north-south direction. In order to investigate the reason behind this observation, further analyses were performed using the stress-strain response of concrete and steel fibers. Stress-strain behavior of steel fibers with corrosion levels 15%, 30%, 40% and 42% are presented in figures 4.16 to 4.19. It can be concluded that with the increasing level of corrosion, reinforcements starts to buckle under compression. This finding is compatible with previous experimental studies focusing on the cyclic behavior of corroded reinforcing bars (Kashani et.al 2013 and Kashani et.al 2015).

It is also important to note that although the target displacements applied to the models with 40% and 42% corrosion levels are same as presented in Table 4.7, when figures 4.18 and 4.19 are compared with each other, a significant change in the stress-strain behavior of reinforcements under compression can be observed. It can be concluded as that the change in the behavior of reinforcing bars under compression was caused by not only increase in target displacement but also change in the buckling behavior. Since increased level corrosion is the primary reason of both increased displacement demand and decreased buckling resistance, it can be claimed that taking the combined effects of changes in demand and capacity due to corrosion of reinforcements into account can be very crucial in order to obtain reliable time-dependent seismic performance evaluations for reinforced concrete buildings.

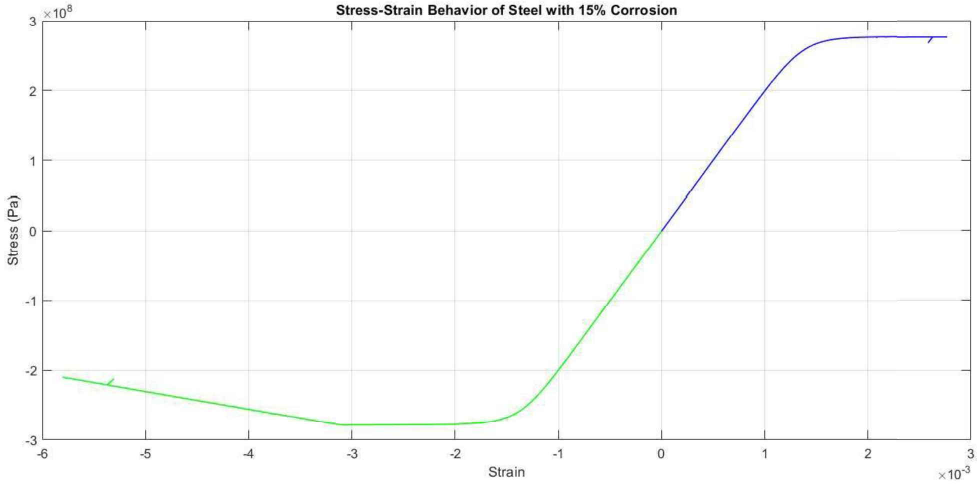

Figure 4.16. Stress-strain behavior of steel with 15% corrosion.

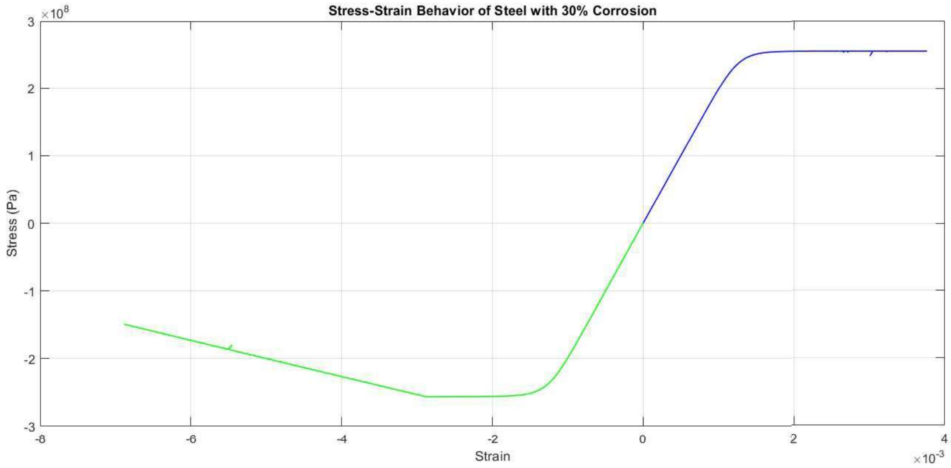

Figure 4.17. Stress-strain behavior of steel with 30% corrosion.

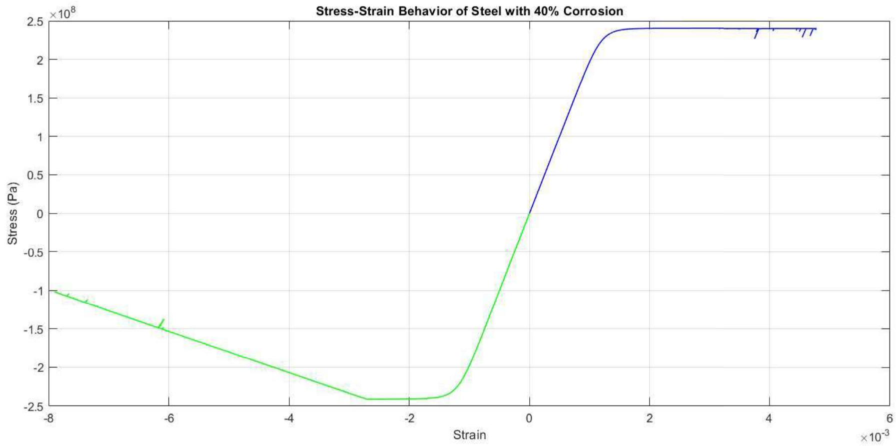

Figure 4.18. Stress-strain behavior of steel with 40% corrosion.

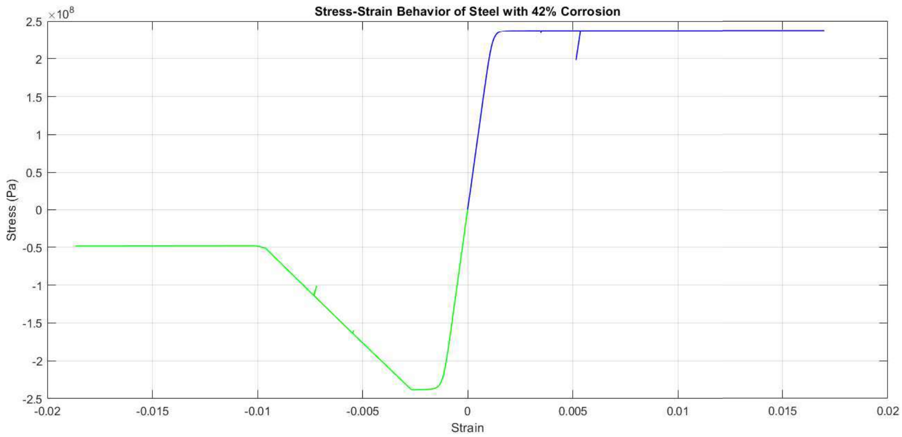

Figure 4.19. Stress-strain behavior of steel with 42% corrosion.

The distributions of the maximum drift ratios are presented in Figures 4.20 and 4.21. It should be noted that the maximum drift ratios through the building height were selected to develop these distributions.

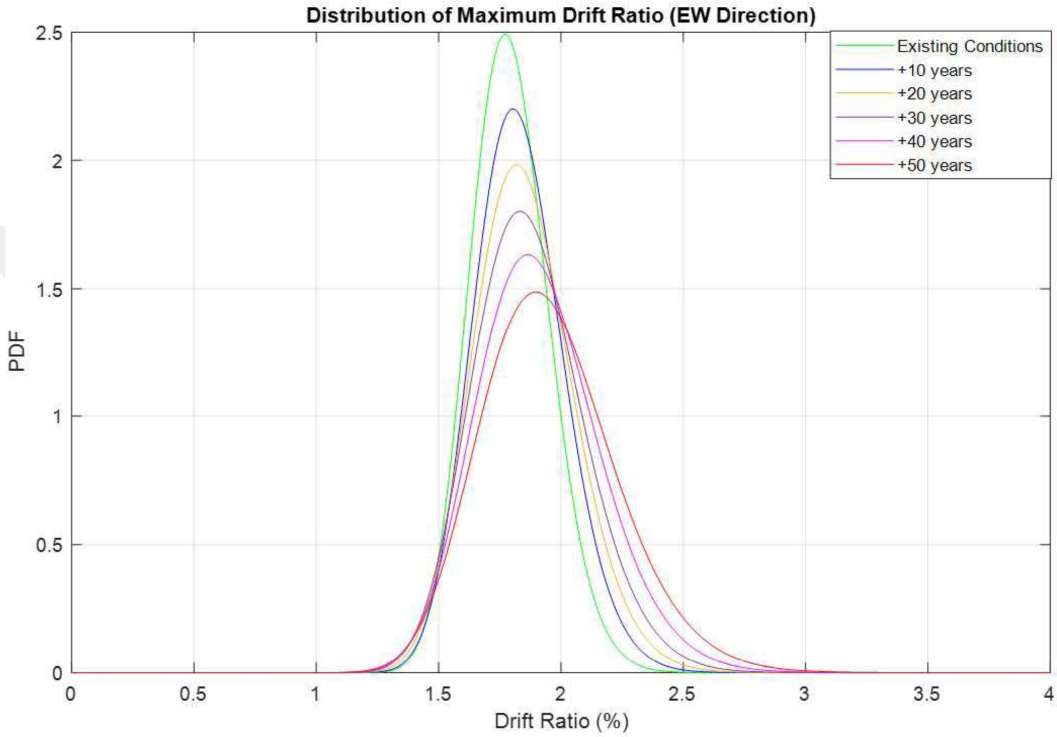

Figure 4.20. Distribution of the maximum drift ratios (east-west direction).

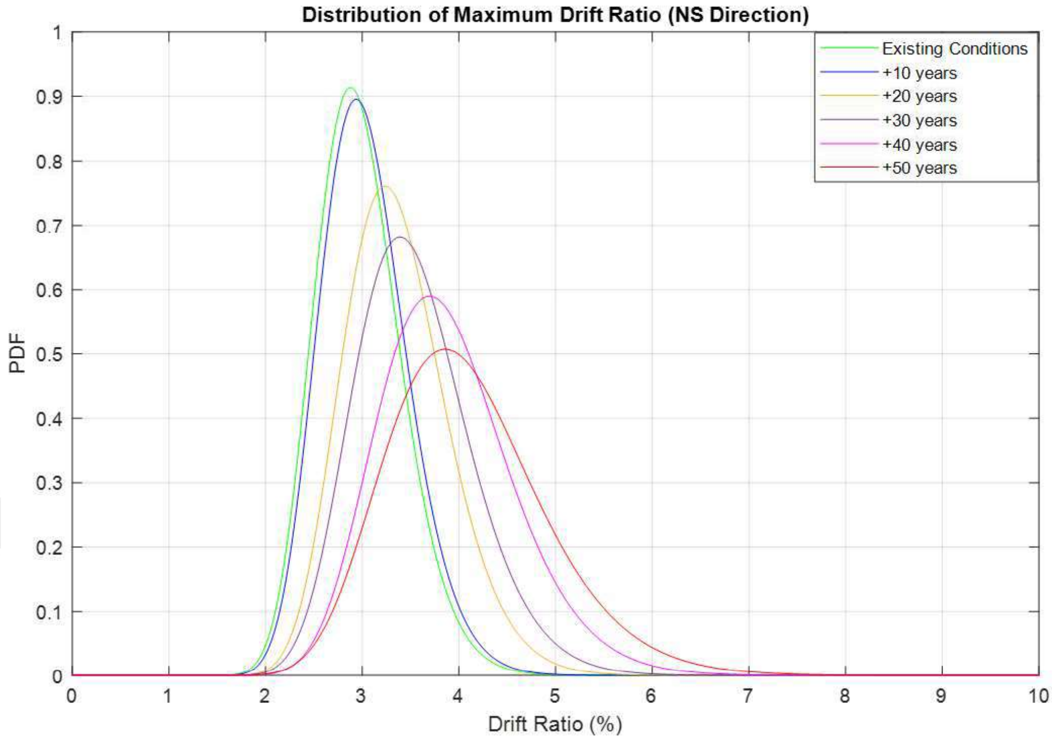

Figure 4.21. Distribution of the maximum drift ratios (north-south direction).

4.5. Time-Dependent Seismic Performance

Time-dependent seismic performance of building was estimated by comparing the drift ratios obtained via nonlinear static analyses with the drift limits for different damage states. In this study, drift limits proposed by FEMA 273 (FEMA 1997) were selected as damage threshold values which are presented in Table 4.8. In order to estimate the damage probability of the building for a defined damage state, cumulative distribution functions shown in Figures 4.22 and 4.23 were used. The cumulative distribution functions present the probability that drift ratios will take a value less that or equal to a selected value. For example, the probability of drift ratios equal to or less than 4 (collapse prevention limit) in North-South direction after 50 years can be determined as 49%. In other word, the probability of having a drift ratio bigger than the collapse prevention threshold value, which is 4, is 51%, which means that the failure probability for collapse prevention damage state in the North-South direction after 50 years equal to 51%. The confidence intervals, which are presented by the dashed lines in Figure 4.23, account for the variability in the fragility estimate related to epistemic uncertainties at the 95% probability level (Contento et.al 2022).

Conducting this evaluation for other time periods, time-variant failure probability of the building can be estimated. Since the performance of the building in North-South direction is more critical in terms of seismic hazards, Figure 4.24 presents the time-variant failure probabilities of the building in this direction. In addition to the failure probabilities obtained from the solid lines in Figure 4.23, confidence intervals determined according to dashed lines are also presented in Figure 4.24 and Table 4.9.

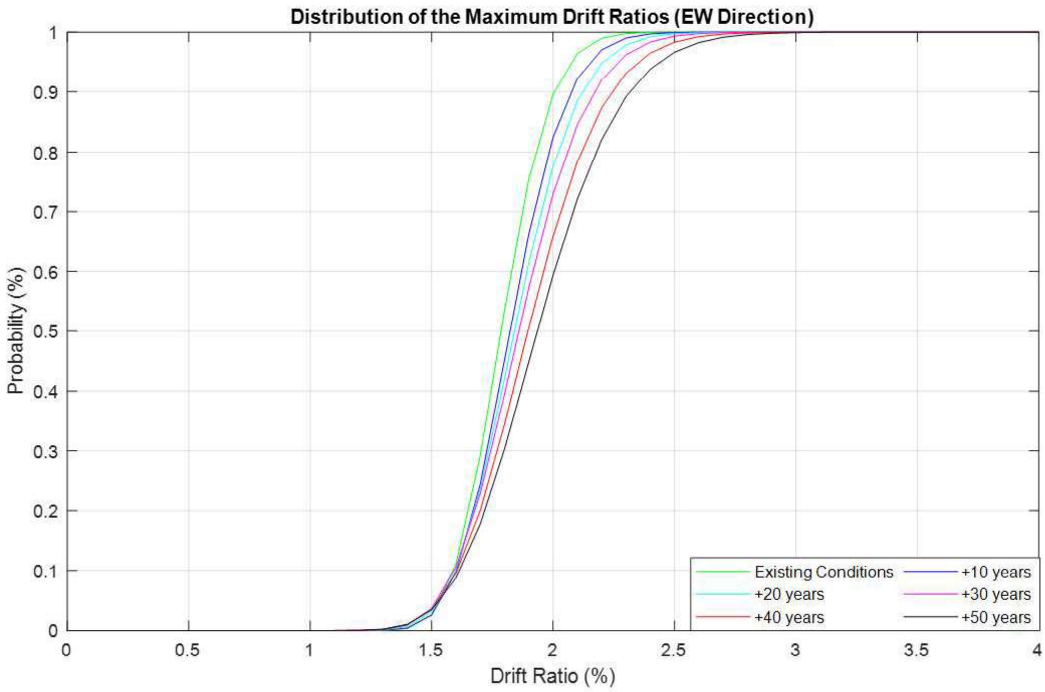

Figure 4.22. Cumulative distribution of the maximum drift ratio in east-west direction.

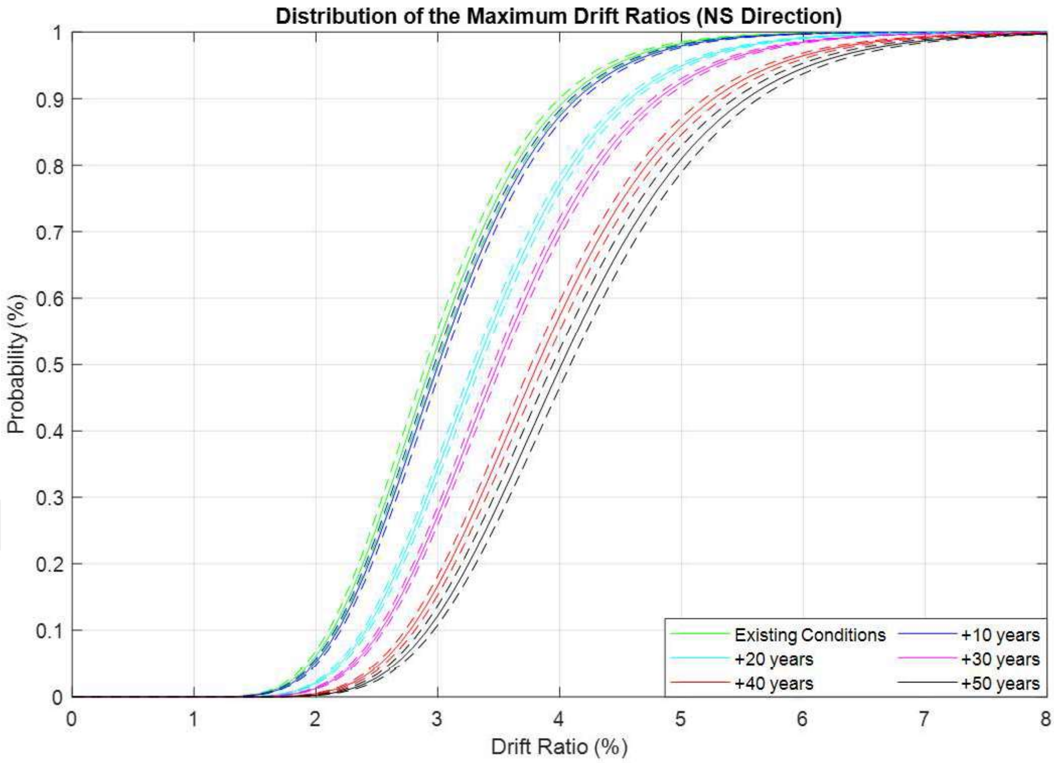

Figure 4.23. Cumulative distribution of the maximum drift ratio in north-south direction.

Table 4.7. Limit state threshold values for inter-story drift ratios.

Damage State	Drift Ratio (%)
Immediate Occupancy	1.00
Life Safety	2.00
Collapse Prevention	4.00

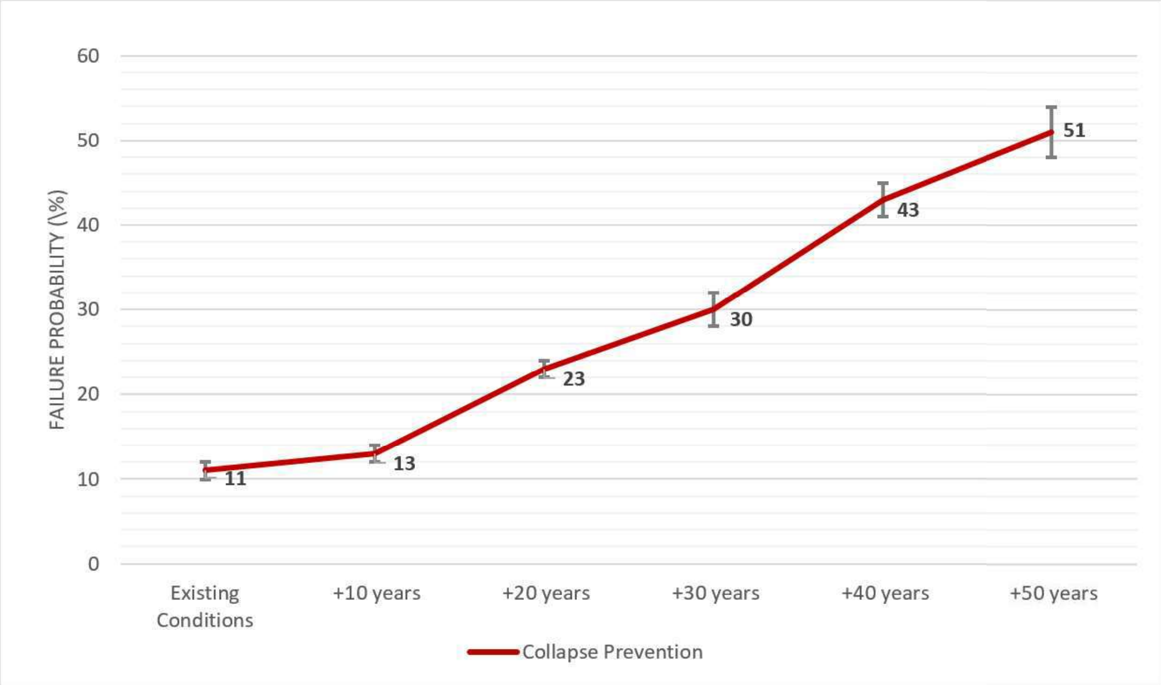

Figure 4.24. Time-variant failure probability of building.

Table 4.8. Time-variant failure probabilities (Collapse Prevention).

Time Period	CI-Lower	Failure Probability	CI-Upper
Existing Condition	10	11	12
+10 years	12	13	14
+20 years	22	23	24
+30 years	28	30	32
+40 years	41	43	45
+50 years	48	51	54

As stated in the Section 1, estimation of the structural performance under seismic excitation is a challenging task due to uncertainties in the seismic demands and the structural capacity to withstand these demands against damage and collapse. It is common in seismic risk estimation to group these uncertainties into two categories which represent the uncertainties stem from factors that are inherently random and uncertainty due to lack of knowledge or ignorance.

The aleatoric uncertainty can be classified as variation in ground motion properties such as the exact location, magnitude and time of future earthquake events whereas epistemic uncertainties in structural capacity estimation are mainly originated from the variation in material and geometric properties.

This study aims to handle uncertainties originated from the changes in material properties of reinforced concrete structures due to adverse effects of corrosion. On the other hand, seismic performances of the building at different time periods were obtained via nonlinear static analyses carried out according to the design spectrum presented in Figure 13. Therefore, it is important to note that the estimated failure probabilities of the building presented in Figure 24 and Table 4.9 are dependent to the design spectrum developed in this study. In other words, in order to include the uncertainties originated from nature of earthquake event, nonlinear time history analysis can be performed using different earthquake records.

5. CONCLUSION

A remarkable number of reinforced concrete buildings are older than 50 years and a notable portion of them is located in seismically active regions such as Greece, Italy, Japan, New Zealand, Turkey and United States. Therefore, to make reliable seismic performance estimations for existing buildings is an inevitable pre-requisite to develop effective strategies to improve the resilience of societies against the earthquake events.

On the other hand, to estimate the structural performance under seismic excitation is a challenging task due to huge uncertainties in the seismic demands and the structural capacity to withstand these demands against damage and collapse. It is common in seismic risk estimation to divide these uncertainties into two categories which represent the uncertainties stem from factors that are inherently random (aleatoric uncertainty) and uncertainty due to lack of knowledge or ignorance (epistemic uncertainty).

The aleatoric uncertainty can be classified as variation in ground motion properties such as the exact location, magnitude and time of future earthquake events. On the other hand, spatial distribution of potential seismic zones, the predicted maximum earthquake magnitude, and the recurrence periods for earthquakes of different magnitudes are continuously being investigated and new models are being developed and updated based on the current and new knowledge to reduce the epistemic part of the uncertainty in future earthquakes.

Epistemic uncertainties in structural capacity estimation are mainly originated from the variation in material and geometric. In addition to variations in the as-built material properties, time-dependent changes in materials due to environmental effects can also be considered as important sources of epistemic uncertainties in structural capacity predictions. Degradation of reinforcing bars due to corrosion under chloride attacks can be one of the main reasons of the deterioration of reinforced concrete structures and it can cause changes in both material and geometric properties such as the reduction of cross sections of reinforcing bars, degradation of the bonds between concrete and reinforcing bars, and cracking of concrete.

Although various aspects of the corrosion have been studied, there is still a lack of information about the relation between the existing corrosion levels and the long-term seismic performance estimation of reinforced concrete buildings.

In this study, Reverse Monte Carlo method is presented to estimate the future corrosion propagation of existing structures. The novelty of the proposed method is to use existing corrosion levels of the reinforcements to make more reliable predictions for the future corrosion propagation. Experimental measurements are used as reference points according to which numerical models used for corrosion prediction can be validated.

As a result, the proposed method can make estimations for the future corrosion levels which comply with the existing corrosion levels on the structure. A case study was performed using the presented method for a corroded reinforced concrete building located in New Zealand, constructed in 1928.

As the first step, the existing corrosion level of the building was used to predict how corrosion can propagate in the future. For this purpose, 10 years time-intervals were considered, and the predictions were made for conditions of the building 10 to 50 years later.

Afterwards, an OpenSees model was developed using the drawings, available information about material properties and the abovementioned corrosion predictions. Nonlinear static analyses were performed for 10 to 50 years later conditions of the building, and the maximum drift ratios were recorded as the performance indicator to carry out seismic performance estimation.

Finally, drift ratio limits provided by FEMA 273 for various damage states were taken as the reference threshold values in order to estimate the time-variant failure probability of the building. It was observed that the increased corrosion levels result in larger drift ratios that result in a significant increase in the failure probability of the building.

As a conclusion, the information about the existing corrosion levels of a building can be a quite valuable input in order to make reliable evaluations for the future seismic performances of the buildings.

6. REFERENCES

Abdul Razak H., and F. C. Choi, 2001, "The Effect of Corrosion on the Natural Frequency and Modal Damping of Reinforced Concrete Beams", *Engineering Structures*, Vol. 23, pp. 1126-1133.

ACI Commitee 318, 2008, "Building Code Requirements for Structural Concrete (ACI 318-08) and Commentary", *American Concrete Institute*, Farmington Hills, MI.

Ahmad, S., 2003, "Reinforcement Corrosion in Concrete Structures, Its Monitoring and Service Life Prediction - a Review", *Journal of Cement and Concrete Composites*, Vol. 25, pp. 459–471.

Alipour, A., B. Shafei, and M. Shinozuka, 2011, "Performance Evaluation of Deteriorating Highway Bridges Located in High Seismic Areas", *Journal of Bridge Engineering*, Vol. 16, pp. 597-611.

Alipour, A., B. Shafei, and M. S. Shinozuka, 2013, "Capacity Loss Evaluation of Reinforced Concrete Bridges Located in Extreme Chloride Laden Environments", *Structure and Infrastructure Engineering*, Vol. 9, pp. 8-27.

Almusallam, A. A. 2001, "Effect of Degree of Corrosion on the Properties of Reinforcing Steel Bars", *Construction and Building Materials*, Vol. 15, pp. 361-368.

Apostolopoulos, C. A. and D. Michalopoulos, 2006, "Effect of Corrosion on Mass Loss, and High and Low Cycle Fatigue of Reinforcing Steel", *Journal of Materials Engineering and Performance*, Vol. 15, pp. 742–749.

Apostopoulos, C. A., and V. G. Papadakis, 2008, “Consequences of Steel Corrosion on the Ductility Properties of Reinforcement Bar”, *Construction and Building Materials*, Vol. 22, pp. 2316-2324.

Astroza R., H. Ebrahimian, J. P. Conte, 2015, ”Material Parameter Identi[U+FB01]cation in Distributed Plasticity FE Models of Frame-Type Structures Using Nonlinear Stochastic Filtering”, *Journal of Engineering Mechanics*, Vol. 141, No. 5, pp. 1-18.

Bal I. E., H. Crowley, and R. Pinho, 2008, ”Displacement-Based Earthquake Loss Assessment for an Earthquake Scenario in Istanbul”, *Journal of Earthquake Engineering*, Vol. 12, pp. 12-22.

Bertolini, L., B. Elsener, P. Pedeferri, and R. Polder, 2004, *Corrosion of Steel in Concrete – Prevention, Diagnosis, Repair*, Wiley-VCH, Weinheim, Germany.

Biondini, F., E. Camnasio, and A. Palermo, 2014, “Lifetime Seismic Performance of Concrete Bridges Exposed to Corrosion”, *Structure and Infrastructure Engineering*, Vol. 10, pp. 880-900.

Biondini, F., E. Camnasio, and A. Titi, 2015, “Seismic Resilience of Concrete Structures under Corrosion”, *Earthquake Engineering and Structural Dynamics*, Vol. 44, pp. 2445-2466.

Biondini, F., and D. M. Frangopol, 2008, “Probabilistic Limit Analysis and Lifetime Prediction Of Concrete Structures”, *Structure and Infrastructure Engineering*, Vol. 4, No. 5, pp. 399-412.

Brown, J. and S. K. Kunnath, 2006, “Uniaxial Material Model for Reinforcing Steel Incorporating Buckling and Low-Cycle Fatigue”, *OpenSees Days 2006*, UC Berkeley.

Bru D., A. Gonzales, F. Jaview Baeza, and S. Ivorra, 2018, "Seismic Behavior of 1960's RC Buildings Exposed to Marine Environment", *Engineering Failure Analysis*, Vol. 90, pp. 324-340.

Choudhury, T., and H.B. Kaushik, 2019, "Treatment of Uncertainties in Seismic Fragility Assessment of RC Frames with Masonry Infill Walls", *Soil Dynamics and Earthquake Engineering*, Vol. 126, p. 105771.

Cicco, A. D., and F. Iesari, 2022, "Advances in Modelling X-Ray Absorption Spectroscopy Data Using Reverse Monte Carlo", *Physical Chemistry Chemical Physics*, Vol. 24, pp. 6988-7000.

Commercial Buildings Energy Consumption Survey, *Commercial Buildings Energy Consumption Survey 2018 Survey Data*,Concrete Preservation Technologies, https://cp-tech.co.uk/, accessed on December 23, 2022.

Contento, A., A. Aloisio, J. Xue, G. Quaranta, B. Briseghella, and P. Gardoni, 2022, "Probabilistic Axial Capacity Model for Concrete-Filled Steel Tubes Accounting for Load Eccentricity and Debonding", *Engineering Structures*, Vol. 268, p. 114730.

Coronelli D. and P. Gambarova, 2004, "Structural Assessment of Corroded Reinforced Concrete Beams: Modelling Guidelines", *Journal of Structural Engineering*, Vol. 130, pp. 1214-1224.

Cui F., H. Zhang, M. Ghosn, and Y. Xu 2018, "Seismic Fragility Analysis of Deteriorating RC Bridge Substructures Subject to Marine Chloride-Induced Corrosion", *Engineering Structures*, Vol. 155, pp. 61-72.

Da, B., Y. Sun, S. F. Mao, Z. M. Zhang, H. Jin, H. Yoshikawa, S. Tanuma, and Z. J. Ding, 2013, “A Reverse Monte Carlo Method for Deriving Optical Constants of Solids from Reflection Electron Energy-Loss Spectroscopy Spectra”, *Journal of Applied Physics*, Vol. 113, No. 21, pp. 1-12.

Dhakal R. P., and K. Maekawa, 2002, “Modeling for Postyield Buckling of Reinforcement”, *Journal of Structural Engineering*, Vol. 128, pp. 1139-1147.

Di Sarno L., and F. Pugliese, 2020, “Numerical Evaluation of the Seismic Performance of Existing Reinforced Concrete Buildings with Corroded Smooth Rebars”, *Bulleting Earthquake Engineering*, Vol. 18, pp. 4227-4273.

Du, Y. G., L. A. Clark, and A. H. C. Chan, 2005, “Effect of corrosion on Ductility of Reinforcing Bars”, *Magazine of Concrete Research*, Vol. 577, pp. 407-419.

Dukes, J., S. Mangalathu, J. E. Padgett, and R. DesRoches, 2018, “Development of a Bridge-Specific Fragility Methodology to Improve the Seismic Resilience Of Bridges”, *Earthquakes and Structures*, Vol. 153, pp. 253-261.

Duvnjak, I., K. Ivan, S. Marijana, and D. Damjanović, 2021, ”Damage Assessment of Reinforced Concrete Elements due to Corrosion Effect using Dynamic Parameters: A Review”, *Buildings*, Vol. 11, No. 1, pp. 1-18.

Economidou, M., 2011, *Europe’s Buildings under the Microscope*, Buildings Performance Institute Europe BPIE, Brussels, Belgium.

www.eia.gov/consumption/commercial/data/2018/index.php?view=characteristicsb6-b10, accessed on 21 December 2022.

Federal Emergency Management Agency, 1997, *NEHRP Guidelines for Seismic Rehabilitation of Buildings*, Federal Emergency Management Agency Report: FEMA 273, Washington D.C., Unites States.

Fernandez, I., J. M. Bairan, and A.R. Mari, 2016, "Mechanical Model to Evaluate Steel Reinforcement Corrosion Effects on σ - ϵ and Fatigue Curves - Experimental Calibration and Validation", *Engineering Structures*, Vol. 118, pp. 320-333.

Fernandez, I., J. M. Bairan, and A. R. Mari, 2015, "Corrosion effects on the Mechanical Properties of Reinforcing Steel Bars. Fatigue and σ - ϵ Behavior", *Construction and Building Materials*, Vol. 101, pp. 772-783.

Fernandez, I., and C. G. Berrocal, 2019, "Mechanical Properties of 30 year-old Naturally Corroded Steel Reinforcing Bars", *International Journal of Concrete Structures and Materials*, Vol.13, No. 9, pp. 1-19.

Fernandez, I., K. Lundgren, and K. Zandi, 2018, "Evaluation of Corrosion Level of Naturally Corroded Bars Using Different Cleaning Methods, Computed Tomography, and 3D Optical Scanning", *Materials and Structures*, pp. 51-78.

Filippidou, F., and J. P. Jimenez Navarro, 2019, *Achieving the Cost-Effective Energy Transformation of Europe's Buildings – JRC Technical Report*, Publications Office of the European Union, Luxembourg, Luxembourg.

Freddi F., V. Novelli, R. Gentile, E. Veliu, S. Andreev, A. Andonov, F. Greco, and E. Zhuleku, 2021, "Observations from the 26th November 2019 Albania Earthquake: the Earthquake Engineering Field Investigation Team (EEFIT) Mission", *Bulletin Earthquake Engineering*, Vol. 19, pp. 2013-2044.

Ghosh, J., and J. E. Padgett, 2010, “Aging Considerations in the Development of Time-Dependent Seismic Fragility Curves”, *Journal of Structural Engineering*, Vol. 136, pp. 1497-1511.

Goksu, C. and A. Ilki, 2016, “Seismic Behavior of Reinforced Concrete Columns with Corroded Deformed Reinforcing Bars”, *ACI Structural Journal*, Vol. 113, pp. 1053 – 1064.

Goksu, C., P. Inci, and A. Ilki, 2016, “Effect of Corrosion on Bond Mechanism between Extremely Low-Strength Concrete and Plain Reinforcing Bars”, *Journal of Performance of Constructed Facilities*, Vol. 30, No. 3, pp. 1-11.

Guo A., H. Li, X. Ba, X. Guan, and H. Li, 2015, “Experimental Investigation on the Cyclic Performance of Reinforced Concrete Piers with Chloride-Induced Corrosion in Marine Environment”, *Engineering Structures*, Vol. 105, pp. 1-11.

Guo, A., W. Yuan, C. Lan, X. Guan, and H. Li, 2015, “Time-Dependent Seismic Demand and Fragility of Deteriorating Bridges for Their Residual Service Life”, *Bulletin of Earthquake Engineering*, Vol. 13, pp. 2389-2409.

Hancilar, U., E. Çaktı, M. Erdik, G. E. Franco, and G. Deodatis, 2014, “Earthquake Vulnerability of School Buildings - Probabilistic Structural Fragility Analyses”, *Soil Dynamics and Earthquake Engineering*, Vol. 67, pp. 169-178.

Hasanzadeh R., R. Ahmadi, M. Eghbali, D. Samadian, and H. Salmanmohajer, 2021, “Reduction of Seismic Resiliency of RC Structures Caused by Chloride Corrosion for Typical School Buildings Located in Hot Climates”, *Structures*, Vol. 34, pp. 4060-4076.

Hastings, W.K., 1970, “Monte Carlo Sampling Methods Using Markov Chains and Their Applications”, *Biometrika*, Vol. 57, pp. 97–109.

Imperatore, S., and Z. Rinaldi, 2019, “Experimental Behavior and Analytical Modeling of Corroded Steel Rebars under Compression”, *Construction and Building Materials*, Vol. 226, pp. 126-138.

Imperatore, S., Z. Rinaldi, and C. Drago, 2017, “Degradation Relationships for the Mechanical Properties of Corroded Steel Rebars”, *Construction and Building Materials*, Vol. 148, pp. 219-230.

Inci, P., C. Goksu, A. Ilki, and N. Kumbasar, 2013, “Effects of Reinforcement Corrosion on the Performance of RC Frame Buildings Subjected to Seismic Actions”, *Journal of Performance of Constructed Facilities*, Vol. 27, pp. 683-696.

Kashani, M. M., A. J. Crewe, and N. A. Alexander, 2013, “Nonlinear Cyclic Response of Corrosion-Damaged Reinforcing Bars with the Effect of Buckling”, *Construction and Building Materials*, Vol. 41, pp. 388-400.

Kashani, M. M., L. N. Lowes, A. J. Crewe, and N. A. Alexander, 2015, “Phenomenological Hysteretic Model for Corroded Reinforcing Bars Including Inelastic Buckling and Low-Cycle Fatigue Degradation”, *Computers and Structures*, Vol. 156, pp. 58-71.

Kashani, M. M., L. N. Lowes, A. J. Crewe, and N. A. Alexander, 2016, “A Multi-Mechanical Nonlinear Fibre Beam-Column Model for Corroded Columns”, *International Journal of Structural Integrity*, Vol. 7, pp. 213-226.

Kaushik H. B. and S. K. Jain, 2007, “Impact of Great December 26, 2004 Sumatra Earthquake and Tsunami on Structures in Port Blair”, *Journal of Performance and Constructed Facilities*, Vol. 21, pp. 128-142.

Konukcu, B. E., H. Karaman, and M. Sahin, 2017, ”Building Damage Analysis for the Updated Building Dataset of Istanbul”, *Natural Hazards*, Vol. 84, pp. 1981–2007.

Kumar, R., and P. Gardoni, 2014, “Effect of Seismic Degradation on the Fragility of Reinforced Concrete Bridges”, *Engineering Structures*, Vol. 79, pp. 267-275.

Lejouad C., B. Richard, P. Mongabure, S. Capdevielle, and F. Ragueneau, 2022, “Assessment of the Seismic Behavior of Reinforced Concrete Elements Affected by Corrosion: An Objective Comparison Between Quasi-Static and Dynamic Tests”, *Structures*, Vol. 39, pp. 653-666.

Liu, X., H. Jiang, and H. Liusheng, 2017, “Experimental Investigation on Seismic Performance of Corroded Reinforced Concrete Moment-Resisting Frames”, *Engineering Structures*, Vol. 153, pp. 639-652.

Li, H., L. Li, G. Zhou, and L. Xu, 2022, “Time-Dependent Seismic Fragility Assessment for Aging Highway Bridges Subject to Non-Uniform Chloride-Induced Corrosion”, *Journal of Earthquake Engineering*, Vol. 267, pp. 3523-3553.

Li, Q., X. Xia, Z. Pei, X. Cheng, D. Zhang, K. Xiao, J. Wu, and X. Li, 2022, “Long-Term Corrosion Monitoring of Carbon Steels and Environmental Correlation Analysis via the Random Forest Method”, *Materials Degradation*, Vol. 6, No. 1, pp. 1-9.

Mazzoni, S., F. McKenna, M. H. Scott, and G. L. Fenves, 2006, *OpenSees: Open System for Earthquake Engineering Simulation. OpenSees Command Language Manual*, CA: Pacific Earthquake Engineering Research Center - University of California, USA.

McGreevy, R. L., 2001, “ Monte Carlo Modelling”, *Journal of Physics: Condensed Matter*, Vol. 13, pp. 877-913.

McKenna F., 2011, ”OpenSees: A Framework for Earthquake Engineering Simulation”, *Computing in Science Engineering*, Vol. 13, No. 4, pp. 58-66.

Meda, A., S. Mostosi, Z. Rinaldi, and P. Riva, 2014, “Experimental Evaluation of the Corrosion Influence on the Cyclic Behaviour of RC Columns”, *Engineering Structures*, Vol. 76, pp. 112-123.

Molina F. J., C. Alonso, and C. Andrade, 1993, “Cover Cracking as a Function of Rebar Corrosion: Part 2- Numerical Model”, *Materials and Structures*, Vol. 26, pp. 532-548.

Müller, C. R., V. Kathriarachchi, M. Schuch, P. Maass, and V. G. Petkov, 2010, “Reverse Monte Carlo Modeling of Ion Conducting Network Glasses - An Evaluation based on Molecular Dynamics Simulations”, *Physical Chemistry Chemical Physics*, Vol. 12, pp. 10444-10451.

NACE/ASTM G193-22, 2022, *Standard Terminology and Acronyms Relating to Corrosion*, ASTM International, Pennsylvania, United States.

Naidu Gopu, G., and S. A. Joseph, ”Corrosion Behavior of Fiber-Reinforced Concrete—A Review”. *Fibers* 2022, Vol. 10, No. 38, pp 1-19.

Nataraj S., L. Hogan, A. Scott, and J. Ingham, 2020, ”Seismic Assessment of Corroded Reinforced Concrete Structures: An Experimental and Prediction Database”, *DesignSafe-CI*, Online.

Nataraj S., L. Hogan, A. Scott, and J. Ingham, 2021, “Simplified Mechanics-Based Approach for the Seismic Assessment of Corroded Reinforced Concrete Structures”, *Journal of Structural Engineering*, Vol. 148, No. 3, pp. 1-18.

Ou, Y. C., and N.D. Nguyen, 2016, “Influences of Location of Reinforcement Corrosion on Seismic Performance of Corroded Reinforced Concrete Beams”, *Engineering Structures*, Vol. 126, pp. 210-223.

Ou, Y. C., Y. T. T. Susanto, and H. Roh, 2016, “Tensile Behavior of Naturally and Artificially Corroded Steel Bars”, *Construction and Building Materials*, Vol. 103, pp. 93-104.

Park, Y. J., A. H. S. Ang, and Y. K. Wen, 1985, “Seismic Damage Analysis of Reinforced Concrete Buildings”, *Journal of Structural Engineering*, Vol. 11, No. 14, pp. 740-757.

Patil, S., B. Karkare, and S. Goyal, 2017, “Corrosion Induced Damage Detection of In-Service RC Slabs Using Acoustic Emission Technique”, *Construction and Building Material*, Vol. 156, pp. 123-130.

Papé T. M. and R. E. Melchers, 2011, “The Effects of Corrosion on 45-year-old Pre-Stressed Concrete Bridge Beams”, *Structure and Infrastructure Engineering*, Vol. 7, pp. 101-108.

Qiu, J. L., and J. X. Gong, 2019, “Analytical Hysteretic Model for Reinforcing Bars”, *Computers and Structures*, Vol. 2014, pp. 48-59.

Rajput, A. S., and U. K. Sharma, 2018, “Corroded Reinforced Concrete Columns under Simulated Seismic Loading”, *Engineering Structures*, Vol. 171, pp. 453-463.

Rao, A. S., M. D. Lepech, and A. Kiremidjian, 2016, “Development of Time-Dependent Fragility Functions for Deteriorating Reinforced Concrete Bridge Piers”, *Structure and Infrastructure Engineering*, Vol. 13, pp. 67-83.

Saatcioglu M. and S. R. Razvi, 1992, “Strength and Ductility of Confined Concrete”, *Journal of Structural Engineering*, Vol. 118, pp. 1590-1607.

Sharma K., L. Deng, and C. C. Noguez, 2016, “Field Investigation on the Performance of Building Structures During the April 25, 2015, Gorkha Earthquake in Nepal”, *Engineering Structures*, Vol. 121, pp. 61-74.

Shinozuka, M., S. H. Kim, S. Kushiyama, and J. H. Yi, 2002, “Fragility Curves of Concrete Bridges Retrofitted by Column Jacketing”, *Earthquake Engineering and Engineering Vibration*, Vol. 12, pp. 195-205.

Singhal, A., and A. S. Kiremidjian, 1996, “Method for Probabilistic Evaluation of Seismic Structural Damage”, *Journal of Structural Engineering*, Vol. 122, No. 12, pp. 1459-1467.

Stewart M. G. and E. Bastidas-Arteaga, 2019, “Corrosion of Concrete and Steel Structures in a Changing Climate”, *Climate Adaptation Engineering*, pp. 99-125.

Strasser F. O., J. J.Bommer, K. Şeşetyan, M. Erdik, Z. Çağnan, J. Irizarry, X. Goula, Lucantoni A., Sabetta F., Bal I. E., Crowley H. and C. Lindholm, 2008, ”A Comparative Study of European Earthquake Loss Estimation Tools for a Scenario in Istanbul”, *Journal of Earthquake Engineering*, Vol. 12, pp. 246-256.

Sucuoglu, H., U. Yazgan, and A. Yakut, 2007, ”A Screening Procedure for Seismic Risk Assessment in Urban Building Stocks”, *Earthquake Spectra*, Vol.23, No. 2, pp. 441-458.

Temleitner, L., 2014, “Structure Determination of Liquid Carbon Tetrabromide via a Combination of X-Ray and Neutron Diffraction Data and Reverse Monte Carlo Modelling”, *Journal of Molecular Liquids*, Vol. 197, pp. 204-210.

Titi, A., S. Bianchi, F. Biondini, and M. Frangopol, 2018, “Influence of the Exposure Scenario and Spatial Correlation on the Probabilistic Life-Cycle Seismic Performance of Deteriorating RC Frames”, *Structure and Infrastructure Engineering*, Vol.

18.

Timoshenko, J., A. Kuzmin, and J. Purans, 2012, "Reverse Monte Carlo Modeling of Thermal Disorder in Crystalline Materials from EXAFS Spectra", *Computer Physics Communications*, Vol. 183, pp. 1237-1245.

Totani, F., A. Aloisio, D. Ranalli, and G. Totani, 2021, "Field Investigation on the Reinforcing Steel Corrosion of RC Infrastructures in Abruzzo", *International Conference of the European Association on Quality Control of Bridges and Structures*, pp. 971-978.

Turkish Seismic Design Code (TSDC), 2018,*Regulations for Buildings to be Constructed in Earthquake Prone Areas*, Ankara, Turkey: TSDC.

Tyagunov, S., M. Pittore, M. Wieland, S. Parolai, D. Bindi, K. Fleming, and J. Zschau, 2014, "Uncertainty and Sensitivity Analyses in Seismic Risk Assessments on the Example of Cologne, Germany", *Natural Hazards and Earth System Sciences*, Vol. 14, pp. 1625–1640.

Van Steen, C., L. Pahlavan, M. Wevers, and E. Verstrynge, 2019, "Localisation and Characterisation of Corrosion Damage in Reinforced Concrete by Means of Acoustic Emission and X-Ray Computed Tomography", *Construction and Building Material*, Vol. 197, pp. 21-29.

Vanama, R. K., and B. Ramakrishan, 2020, "Improved Degradation Relations for the Tensile Properties of Naturally And Artificially Corroded Steel Rebars", *Construction and Building Materials*, Vol. 249, pp. 118706-118727.

Vu, N. S., and B. Li, 2018, "Seismic Performance of Flexural Reinforced Concrete Columns with Corroded Reinforcement", *ACI Structural Journal*, Vol. 115, pp. 1253-1266.

Wen, Y. K., B. R. Ellingwood, D. Veneziano, and J. Bracci, 2003, *Uncertainty Modeling in Earthquake Engineering*, MAE Center, Department of Civil Environmental Engineering, University of Illinois, Urbana-Champaign, United States.

Yakut A., H. Sucuoglu, and S. Akkar, 2012, "Seismic Risk Prioritization of Residential Buildings in Istanbul", *Earthquake Engineering and Structural Dynamics*, Vol. 41, No. 11, pp. 1533-1547.

Yuan, Z., C. Fang, M. Parsaeimaram, and S. Yang, 2017, "Cyclic Behavior of Corroded Reinforced Concrete Bridge Piers", *Journal of Bridge Engineering*, Vol. 22, No. 7, pp. 1-21.

Yuan, W., A. Guo, and H. Li, 2017, "Experimental Investigation on the Cyclic Behaviors of Corroded Coastal Bridge Piers with Transfer of Plastic Hinge due to Non-Uniform Corrosion", *Soil Dynamics and Earthquake Engineering*, Vol. 102, pp. 112-123.

Yuan, W., A. Guo, W. Yuan, and H. Li, 2018, "Shaking Table Tests of Coastal Bridge Piers with Different Levels of Corrosion Damage Caused by Chloride Penetration", *Construction and Building Materials*, Vol. 173, pp. 160-171.

Zanini, M. A., F. Faleschini, and C. Pellegrino, 2017, "Probabilistic Seismic Risk Forecasting of Aging Bridge Networks", *Engineering Structure*, Vol. 136, pp. 219-232.

Zanini, M. A., C. Pellegrino, R. Morbin, and C. Modena, 2013, "Seismic Vulnerability of Bridges in Transport Networks Subjected to Environmental Deterioration", *Bulletin of Earthquake Engineering*, Vol. 11, pp. 561-579.

Zhang, P. S., M. Lu, and X. Y. Li, 1995, "The Mechanical Behaviour of Corroded Bar", *Journal of Industrial Buildings*, pp. 25-41.

Zhang, W., X. Song, X. Gu, and S. Li, 2012, “Tensile and Fatigue Behavior of Corroded Rebars”, *Construction and Building Materials*, Vol. 34, pp. 409-417.

Zheng, Y., Y. Zhou, Y. Zhou, T. Pan, L. Sun, and D. Liu, 2020, “Localized Corrosion Induced Damage Monitoring of Large-Scale RC Piles using Acoustic Emission Technique in the Marine Environment”, *Construction and Building Material*, Vol 243, p. 118270.

Zhong, J., Y. Pang, J. S. Jeon, R. DesRoches, and W. Yuan, 2016, “Seismic Fragility Assessment of Long-Span Cable-Stayed Bridges in China”, *Advances in Structural Engineering*, Vol. 19, No. 11, pp. 1-16.